醫學博士 學位論文

The role of SCAMP5 in modulating synaptic vesicle endocytosis during neuronal activity

신경활성상태에서 SCAMP5을 통한 시냅스낭 순환과정에 대한 조절기전

2015 年 2 月

서울大學校 大學院

醫科學科 醫科學專攻

趙 海 燕

The role of SCAMP5 in modulating synaptic vesicle endocytosis during neuronal activity

2015

赵海燕

醫學博士 學位論文

신경활성상태에서 SCAMP5을 통한 시냅스낭 순환과정에 대한 조절기전

The role of SCAMP5 in modulating synaptic vesicle endocytosis during neuronal activity

2015 年 2月

서울大學校 大學院

醫科學科 醫科學專攻

趙 海 燕

A thesis of the Degree of Doctor of Philosophy

The role of SCAMP5 in modulating synaptic vesicle endocytosis during neuronal activity

신경활성상태에서 SCAMP5을 통한 시냅스낭 순환과정에 대한 조절기전

December, 2014

The Department of Biomedical Sciences

Seoul National University

College of Medicine

Hai Yan Zhao

신경활성상태에서 SCAMP5을 통한 시냅스낭 순환과정에 대한 조절기전

지도교수 장 성 호

이 논문을 의학박사 학위논문으로 제출함

2014년 10월

서울대학교 대학원

의과학과 의과학전공

趙 海 燕

趙海燕의 의학박사 학위논문을 인준함

2014년 12월

위 원 장 _____ (인)

부위원장 _____ (인)

위 원 _____ (인)

위 원 _____ (인)

위 원 _____ (인)

The role of SCAMP5 in modulating synaptic vesicle endocytosis during neuronal activity

by
Hai Yan Zhao M.D.

A thesis submitted to the Department of Biomedical Sciences in partial fulfillment of the requirement of the Degree of Doctor of Philosophy in Biomedical Sciences at Seoul National University College of Medicine

December, 2014

Approved by Thesis Committee:

Professor _____ **Chairman**

Professor _____ **Vice chairman**

Professor _____

Professor _____

Professor _____

ABSTRACT

The role of SCAMP5 in modulating synaptic vesicle endocytosis during neuronal activity

Hai Yan Zhao

Department of Biomedical Sciences

The Graduate School

Seoul National University

Neurotransmitter release is the key process to initiate synaptic transmission at the presynaptic nerve terminal. Upon stimulation, synaptic vesicles (SVs) that contain neurotransmitters exocytose and fuse with the plasma membrane to release neurotransmitters. To maintain continuous synaptic transmission, once fused SVs should be recycled with endocytosis. Although several synaptic vesicle proteins have been implicated in these events, their precise function in SV trafficking remain largely elusive.

Secretory carrier membrane proteins (SCAMPs) are tetraspan vesicle

membrane proteins. SCAMPs are comprised of an N-terminal tail (N-term), four transmembrane regions (TM1-4), the loop region between TM2 and TM3 (2/3 loop) and C-terminal cytoplasmic tail (C-term). Among five currently known isoforms of SCAMPs (SCAMP1-5), SCAMP1-4 are ubiquitously expressed while SCAMP5 is mainly expressed in the brain and is highly abundant in SVs. SCAMPs 1-3 are known to play not only in regulation of fusion pore formation during dense-core vesicle (DCV) secretion in PC12 cells at the plasma membrane but also in trafficking events in the trans-golgi network (TGN) and endosomal recycling compartment, suggesting their fundamental function in vesicular traffic. Recently SCAMP5 is identified as a candidate gene for autism and its expression is found to be reduced to < 40% in a patient with idiopathic, sporadic autism. Moreover, SCAMP5 expression is also found to be markedly increased in the striatum of Huntington's disease. Therefore, the change in the expression of SCAMP5 may be related to the synaptic dysfunction observed in these diseases, but none is known for SCAMP5 role at the synapse so far.

The aim of the present study is to reveal the role of SCAMP5 in presynaptic function. For this purpose, I used SCAMP5-specific shRNAs to knock down (KD) endogenous expression of SCAMP5 in cultured rat hippocampal neurons. Here, I found that SCAMP5 KD induced reduction in total SVs pool size concomitant with decreases in both recycling and resting pool size but the ratio of recycling/resting pool was significantly increased. I also found that although exocytotic kinetics was unaffected by SCAMP5 KD, SCAMP5 KD

slowed down endocytosis after stimulation but the most severely impaired was SV endocytosis during stimulation.The endocytic defects were independently verified using FM1-43. I further found that SCAMP5 KD dramatically lowered the threshold of activity at which SV endocytosis became unable to compensate for the ongoing exocytosis occurring during stimulation. The endocytosis defect in SCAMP5 KD was rescued by co-expression of shRNA-resistant SCAMP5. To find out which domain(s) of SCAMP5 is responsible for endocytosis regulation, I overexpressed N-term, 2/3 loop, or C-term and found that overexpression SCAMP5 N-term led to slower endocytosis during strong stimulation which is similar to the endocytosis defects found in SCAMP5 KD. In addition, I found that SCAMP5 binds to the AP-2 through its N-terminal YXXΦ motif. Accordingly, overexpression of N-term YXXΦ point mutant (Y22A) failed to induce endocytic defects during stimulation.

In summary, my results suggest that SCAMP5 mainly functions during high neuronal activity when a heavy load is imposed on endocytosis. Considering recent findings in which SCAMP5 expression is either increased or decreased in Huntington disease or autism patient, my data also raise the possibility that a reduction or an increase of SCAMP5 expression in Huntington or autism patient may be related to synaptic dysfunction observed in each disease.

* The part of this work has been published in *J Neurosci* (Zhao H, et al. SCAMP5 plays a critical role in synaptic vesicle endocytosis during high neuronal activity. J Neurosci.2014 Jul 23; 34(30):10085-95)

Keywords: neuronal activity, recycling pool, resting pool, SCAMP5, synaptic vesicle endocytosis.

Student Number: 2010-24179

CONTENTS

LIST OF FIGURES

LIST OF ABBREVIATIONS

SCAMPs, Secretory carrier membrane protein

SV, Synaptic vesicle

KD, Knockdown

OE, Overexpression

shRNA, Small hairpin RNA

DCV, Dense-core vesicle

TGN, Trans-Golgi network

vGpH, vGlut1-pHluorin

SypHy, Synaptophysin-pHluorin

AAV, Adeno-associated virus

APs, Action potentials

Baf, Bafilomycin A1

AP-2, Adaptor protein complex 2

AP-180, Adaptor protein complex 180

DIV, Days in vitro

CCP, Clathrin–coated pit

Syn, Synapsin

ASD, Autism spectrum disorders

HD, Huntington's disease

The role of SCAMP5 in modulating synaptic vesicle endocytosis during neuronal activity

INTRODUCTION

Synaptic vesicle release and clathrin mediated endocytosis

The presynaptic nerve terminal is a crucial component of neurotransmitter and synaptic vesicle (SV) release. Upon stimulation, SVs fuse with the presynaptic membrane and release the neurotransmitter through exocytosis, whereby the neurons communicate with neighboring cells. After exocytosis, the SV proteins and lipids are returned and restored to the SVs via endocytosis. Clathrin-mediated endocytosis (CME) is known to be the major endocytic pathway for SV retrieval. During this process, endocytic proteins are assembled to phosphatidylinositol 4,5-bisphosphate (PIP_2) enriched plasma membrane, which recruits AP-2, epsin, AP-180, clathrin and synaptotagmin (1). Followed by the protein accumulation, membrane invagination and clathrin–coated pit (CCP) maturation begins with the endocytic proteins, such as endophilin, synaptojanin, actin, and amphiphysin (2, 3). Subsequently, dynamin, a GTPase protein is recruited around the neck of CCP, pinches off the neck to complete membrane scission (4-10). Finally, auxilin, hsc70 and synaptojanin are involved in uncoating clathrin from the SVs (11).

The SV components such as the endocytosis-related protein (14), the cytoskeletal protein (15), the transporter, and channel proteins are recycled through various protein-protein interactions in the presynaptic nerve terminals, and the previous studies reported some of the key mechanisms involved in

this process (14, 15). Evidently, SVs recycling events are extremely important for restocking the neurotransmitters and preventing depletion of SV during sustained release.

Secretory Carrier Membrane Proteins

Secretory carrier membrane proteins (SCAMPs) are secretory vesicle components found in exocrine glands (18, 19). Among the five identified SCAMPs (SCAMPs 1 to 5), SCAMPs 1 to 3 share a common domain structure that is comprised of a cytoplasmic N-terminal domain with multiple endocytic NPF repeats, four highly conserved transmembrane regions, and a short cytoplasmic C-terminal tail. It is well-known that the N-terminal NPF repeats domain binds to the EH domain proteins that are involved in clathrin-mediated vesicle budding either from the plasma membrane or the trans-Golgi network (TGN) (17). SCAMPs 4 and 5 lack the N-terminal NPF repeats and are thus assumed to not function in endocytosis (16). According to the previous studies, at least one of five SCAMP isoforms is present in secretory organelar membranes and recycling vesicles in cells (18, 19).

Using the RNA-blotting method, another study found that SCAMP1 to 4 are ubiquitously expressed, whereas SCAMP5 is brain specific (16). In addition, SCAMP1 and 5 are highly abundant in SVs, whereas SCAMP5 is the only isoform that is restrictively expressed in the brain (16). SCAMP1 to 3 are known to play roles in fusion pore formation in the plasma membrane during dense-core vesicle (DCV) secretion in PC12 cells, as well as in trafficking events in the TGN and endosomal recycling compartment (20-28).

Since SCAMP1 and 5 are highly abundant in SVs and SCAMP1 interacts with intersection and γ-synergin, which are the EH domain-containing proteins that are involved in endocytosis, SCAMP1 was assumed to play an important role in synaptic physiology. The data from SCAMP1 knock-out mice, however, have shown that it is not essential for synaptic functions and does not affect survival or basic brain function (20). This raises the possibility that other brain specific SCAMPs, SCAMP5, might be active. Besides, SCAMP5 is the most highly expressed in nervous tissue (17) and is undetectable in neuroendocrine glands, which express many other neuron-specific proteins, such as synaptophysin and synaptotagmin (18). This suggests a selective role for SCAMP5 in SV trafficking, but evidence for this has been mostly lacking.

Correlation of neurological diseases and SCAMP5

Recent study showed that SCAMP5 expression is markedly increased in the striatum of Huntington's disease patients and that its down-regulation alleviates ER stress-induced protein aggregation in huntingtin mutants and the inhibition of endocytosis (29). SCAMP5 is also highly correlative with calcyon (30), which is implicated in schizophrenia, and Attention Deficit/Hyperactivity Disorder (ADHD) (31-33). Another study on brain tumor tissues showed that SCAMP5 is correlated with the microRNA-mRNA pairs, which have a strong relationship with the carcinogenesis gene in brain tumors (34). Another study found that SCAMP5 gene expression increases

when exposed to methylazoxymethanol, a well-known and widely used developmental neurotoxin, in cultured mouse neurons (35). In addition, SCAMP5 is a sensitive protein marker for neuroendocrine lung cancer and is related the Lambert-Eaton Myasthenia syndrome, a presynaptic disorder of neuromuscular transmission (36). A recent study also identified SCAMP5 as a candidate gene for autism, showing that it was silenced on a derivative chromosome and that its expression was reduced to less than < 40% in a patient with idiopathic, sporadic autism (37).

High correlation between various neurological diseases and SCAMP5 expression strongly suggest its importance in nervous function but none has been reported so far.

The importance of current study

I found that the knockdown of endogenous SCAMP5 by SCAMP5-specific shRNAs leads to a reduction in both total vesicle pool size, and recycling pool size, but the recycling/resting pool ratio was significantly increased. When I investigated the role of SCAMP5 KD in SV recycling, I found that most severly impaired was SV endocytosis during strong stimulation. Thus, my results suggest that SCAMP5's function is to control the SV recycling machinery during high levels of neuronal activity.

I further found that SCAMP5 binds to AP-2. AP-2 interacts with clathrin and many of the accessory proteins, such as eps15, AP180, epsin, amphiphysin and synaptojanin (1). My results therefore strongly suggest that SCAMP5

functions as a hub for interactions during CCP formation in the CME. Without SCAMP5, endocytic complex recruitment by AP-2/SCAMP5 is limited especially during intense neuronal activity, SVs reformation by endocytosis therefore would be limited (38, 39). This highlights the importance of the AP-2 and SCAMP5 interaction. Further study for additional molecular mechanisms of synaptic dysfunction in SCAMP5 KD neurons need to be required.

MATERIAL AND METHODS

DNA constructs

SCAMP5 (GeneID: 65171) was purchased from SuperScritp™ rat brain cDNA library (Invitrogen), amplified by PCR and subcloned into pEGFP (Clontech), mCherry (generously provided by Dr. Roger Y. Tsien at University of California-San Diego) and HA vector. The following constructs were PCR amplified and subcloned into expression vectors: SCAMP5-Nterm domain (residues 1-189), SCAMP5 2/3loop (residues 211-402), SCAMP5-Cterm (residues 435-708). The fidelity of all constructs was verified by sequencing. vGlut1-pHluorin (vGpH), synaptophysin-pHluorin (SypHy), and synaptopHluorin were kindly provided by Dr. John Rubenstein at University of California-San Francisco, Dr. Leon Lagnado at the Medical Research Council, and Dr. James Rothman at Sloan Kettering Cancer Center, respectively.

Antibodies and reagents

The following antibodies were used: anti-SCAMP5 antibody that does not recognize SCAMP1 was form Sigma (catalog #S0943, St. Louis, MO), anti-SCAMP1 antibody (catalog #121002), anti-synaptophysin antibody (#101011), and anti-synaptobrevin antibody (catalog #104211) were from SYSY（Goettingen, Germany), anti-AP2μ2 antibody were from BD biosciences (catalog #611350), anti-tubulin antibody, anti-GFP antibody, and

anti-β tubulin antibody were from Abcam (Cambridge, UK). Secondary antibodies were obtained from Jackson ImmunoResearch (West Grove, PA). Bafilomycin A1 was from Calbiochem (San Diego, CA) and all other reagents were from Sigma.

Neuron culture and transfection

Hippocampal neurons derived from embryonic day 18 Sprague Dawley fetal rats were prepared as described (40).The first phase of operation, hippocampi were dissected from, dissociated with papain, and triturated with a polished half-bore Pasteur pipette. The cells (2.5×10^5) in minimum Eagle's medium (Invitrogen), supplemented with 0.6% glucose, 1 mM pyruvate, 2 mM L-glutamine, 10% fetal bovine serum (Hyclone, Logan, UT, USA), and antibiotics were plated on poly-D-lysine-coated glass coverslips in a 60-mm Petri dish. Four hours after plating, the medium was replaced with Neurobasal (Invitrogen) supplemented with 2% B-27, 0.5 mM L-glutamine. 4 μM of 1-β-D-cytosine-arabinofuranoside (Ara-C, Sigma) was added as needed. Neurons were transfected using a modified calcium-phosphate method (41). In order to implement these transfection methods, briefly prepare, 6 μg of cDNA and 9.3 μl of 2 M $CaCl_2$ were mixed in distilled water to a total volume of 75 μl, and same volume of 2 x BBS was added. The cell culture medium was completely replaced by transfection medium (MEM, 1 mM pyruvate, 0.6% glucose, 10 mM glutamine, and 10 mM HEPES, pH 7.65), and the cDNA mixture was added to the in vitro cultured neuron, and incubated in a 5% CO_2 incubator for

90 min. Cells were washed twice with washing medium (pH 7.35) and then returned to the original culture medium. vGpH or SypHy and pU6mRFP constructs were cotransfected in a ratio of 5:1.

Immunoblot analysis at hippocampal neuron

Hippocampal neurons (~300.000) were plated on 10-mm tissue culture dishes coated with poly-D-lysine and grown for 3, 7, 14, 18 or 21 days. They were lysed in a lysis buffer containing the following (in mM): 1 sodium orthovanadate, 10 NaF, 10 Tris-HCl, pH 7.4, 1 PMSF, 10 leupeptin, 1.5 pepstatin, 1 aprotinin and scratch out. The sample was then transferred to 37°C water bath incubated for 15min, and clarified centrifugation at 13,000 x g for 10 min. Protein concentrations were measured with a bicinchoninic acid protein assay reagent kit (Thermo Fisher Scientific, Waltham, MA). Constant amounts of proteins were separated on SDS-PAGE and transferred to poly-vinylidene di fluoride membranes (Bio-Rad). The membranes were blocked for 1 h with 5% nonfat dry milk in TBST (10 mM Tris-HCl, pH 7.5,100 mM NaCl, and 0.1% Tween 20) incubated with the respective primary antibodies, anti-SCAMP5, anti-tubulin and then with horseradish peroxidase-conjugated secondary antibody (Jackson ImmunoResearch). The antigen-antibody complexes were detected with enhanced chemiluminescence (ECL) reagents (Abclon, Seoul, Korea).

SCAMP5 knock-down by shRNA

SCAMP5-specific small hairpin RNA (shRNA) was designed from the rat SCAMP5 cDNA sequence (NM_031726) targeting to the region of nucleotides 5'-GCCATGTTTCTACCAAGACTT-3'(shRNA#1, nucleotides 54-74) and 5'-GCATGGTTCATAAGTTCTA-3'(shRNA#2, nucleotides 509-527). A pair of complementary oligonucleotides was synthesized separately with the addition of an ApaI enzyme site at the 5'end and an EcoRI site at the 3'end. The annealed cDNA fragment was cloned into the ApaI-EcoRI sites of pSilencer 1.0-U6 vector (Ambion, Austin, TX) modified by inserting an mRFP at the C-terminus. For evading RNA interference, silent mutations within shRNA#2 targeting sequence (T516C, T519C and C525T) in HA-SCAMP5 were generated using QuickChange site-directed mutagenesis kit (Stratagene, Austin ,Texas). The fidelity of all constructs was verified by sequencing. shRNA#2 sequences was cloned into the pAAV-U6 shRNA vector using BamHI/SalI sites, and AAV vectors were produced by KIST virus facility (Seoul, Korea) by co-transfecting each pAAV vector with the pAAV-RC1 and pHelper vector (Cell Biolabs, San Diego, CA) in the 293FT packaging cell line. The supernatant was collected and concentrated by ultracentrifugation.

Knockdown efficiency was examined in GFP-SCAMP5 expressed HEK293T cells and cultured hippocampal neurons by Western blotting. Cells were cultured at 37^{o}C and 5% CO_2 in Dulbecco's modified Eagle's medium (Invitrogen) supplemented with 10% fetal bovine serum and transfected with

GFP-SCAMP5 and shRNAs using Lipofectamine 2000. Cells were examined for transfection efficiency after 16-24 h under a fluorescence microscope. For Western blotting, HEK293T cells or AAV-infected hippocampal neurons were lysed in a lysis buffer containing the following (in mM): 1 sodium orthovanadate, 10 NaF, 10 Tris-HCl, pH 7.4, 1 PMSF, 10 leupeptin, 1.5 pepstatin, and 1 aprotinin along with 1% SDS, clarified by centrifugation 15,000 x g for 10 min, and incubated for 15min in 37^{o}C water bath . Protein concentrations were measured with a bicinchoninic acid protein assay reagent kit. Samples containing 100 μg of total protein were separated on SDS-PAGE and transferred to poly-vinylidene di fluoride membranes. The membranes were blocked for 1 h with 5% nonfat dry milk in TBST (10 mM Tris-HCl, pH 7.5,100 mM NaCl, and 0.1% Tween 20) incubated with the respective primary antibodies, for 2 h at room temperature. After extensive washing in TBST, the membrane was incubated with horseradish peroxidase-conjugated secondary antibody. The antigen-antibody complexes were detected with enhanced chemiluminescence (ECL) reagents. shRNA#2 was used to knock down the expression of SCAMP5 in all of the experiments expect for shown in Figure 8, in which shRNA#1 was used.

Synaptic vesicle pool size measurement

To estimate the size of each fraction of SV pool, vGpH-transfected neurons at 16 d *in vitro* were stimulated with 900 action potentials (APs) at 10 Hz in the presence of 0.5 μM bafilomycin A1(*Baf*) to release entire recycling pool of

SVs(42). *Baf* was dissolved in Me_2SO to 0.2 mM and diluted to a final concentration of 0.5 μM prior to the experiments. *Baf* was applied throughout the experiments. The changes of the in fluorescence intensity to the plateau reflects the entire recycling pool. The resting pool that cannot be mobilized by neuronal activity can be uncovered by applying NH_4Cl solution to unquench all acidic vesicles that have not been released. Fluorescence intensity was normalized to the maximum fluorescence change after NH_4Cl treatment. Data were collected from 30 to 40 boutons of 12–24 neurons in each coverslip and "n" stands for the number of coverslip. Data are presented as means ± SE. Statistical analysis was carried out with SPSS Version 19 software (IBM, Armonk, NY). For multiple conditions, means were compared by ANOVA followed by Tukey's HSD *post hoc* test.

vGpH (or SypHy) exo/endocytosis assay and image analysis

Coverslips were mounted in a perfusion/stimulation chamber equipped with platinum-iridium field stimulus electrodes (Chamlide EC, LCI, Seoul, Korea) on the stage of an Olympus IX-71 inverted microscope with 40 X, 1.0 NA oil lens. The cells were continuously perfused at room temperature with Tyrode solution containing the following (in mM): 136 NaCl, 2.5 KCl, 2 $CaCl_2$, 1.3 $MgCl_2$, 10 HEPES, and 10 glucose, pH 7.3; 10 μM 6-cyano-7-nitroquinoxaline-2, 3-dione was added to the imaging buffer to reduce spontaneous activity and prevent recurrent excitation during stimulation.

Time-lapse images were acquired every 5 s for 4 min using a back-illuminated Andor iXon 897 EMCCD camera (Andor Technologies, Belfast, Northern Ireland) driven by MetaMorph Imaging software (Molecular Devices, Sunnyvale, CA). From the fourth frame, the cells were stimulated (1 ms, 20-50 V, bipolar) using an A310 Accupulser current stimulator (World Precision Instruments, Sarasota, FL). Quantitative measurements of the fluorescence intensity at individual boutons were obtained by averaging a selected area of pixel intensities using ImageJ program. Individual regions were selected by hand, and rectangular regions of interest were drawn around the synaptic boutons, and average intensities were calculated. Large puncta, typically representative of clusters of smaller synapses, were rejected during the selection procedure. The center of intensity of each synapse was calculated to correct for any image shift over the course of the experiment. Fluorescence was expressed in intensity units that correspond to fluorescence values averaged over all pixels within the region of interest. All fitting was done using individual error bars to weight the fit, using Origin 8 (OriginLab Corporation, Northampton, MA). To obtain the endocytic time constant after stimulation, the decay of vGpH after stimulation was fitted with a single exponential function. In some experiments in which fluorescence decay does not decay to zero (as in the case of SCAMP5 KD), the time constant was obtained using the initial slope method. In this method, a line is drawn from the initial point at the initial slope and where that line intersects the final value is the time constant.

For exocytosis assays, neurons were preincubated with *Baf* for 60 s to block

the reacidification and stimulated for 120 s at 10 Hz, which is known to deplete total recycling pool of vesicles(42, 43). Net fluorescence changes were obtained by subtracting the average intensity of the first four frames (F_0) from the intensity of each frame (F_t) for individual boutons, normalizing to the maximum fluorescence intensity (F_{max} - F_0), and then averaging. To get endocytic rate during stimulation, neurons were stimulated in the presence or absence of *Baf*. In the absence of *Baf*, the fluorescence signal reflects the net balance of exocytosis and endocytosis ($\Delta F_{exo-endo}$). In the presence of *Baf*, exocytosis events are trapped in an alkaline state, and the fluorescence signal reflects exocytosis (ΔF_{exo}). Fluorescence values were normalized to the peak fluorescence in each experimental condition. Endocytosis during stimulation was derived by subtracting the vGpH or SypHy fluorescence in the absence of *Baf* from that in the presence of *Baf* ($\Delta F_{endo} = \Delta F_{exo} - \Delta F_{exo-endo}$). The traces were normalized to the maximum stable fluorescence signal after *Baf* treatment. Rate of exocytosis and rate of endocytosis during stimulation were obtained from the linear fits to the data during a 300 AP stimulus. Photobleaching drift was corrected empirically either using local background or time-lapse imaging without stimulation before the experiments. Because both yielded similar results (and actually prebleaching sometimes damaged the cells), we only use local background method throughout the study. We selected the regions where blurred fluorescence signals are observed as well as where no active changes in fluorescence intensity are observed during experiments. We took decay kinetics of these local backgrounds by fitting a double exponential function to local background decay signal and then

subtracting this function from the original trace. The result was a trace with a relatively flat baseline. Data were collected from 30–40 boutons of 12–24 neurons in each coverslip and "n" stands for the number of coverslip. Statistical analysis was carried out with SPSS version 19. For multiple conditions, we compared means by ANOVA followed by Tukey's HSD *post hoc* test or Fisher's LSD test (depending on the number of groups). For acidification assay, neurons were mounted in a rapid perfusion chamber (Chamlide CF, LCI) equipped with platinum-iridium electrodes. The extracellular buffer was changed twice from pH 7.4 to 5.3 and back before and after 300 APs at 10 Hz.

FM 1-43 uptake assay

Pools of synaptic vesicles were labeled during electrical stimulation for 30 s at 10 Hz in the presence of 10 μM FM 1-43 (Invitrogen). FM 1–43 was loaded with the onset of stimulation (300 APs) and immediately washed out with the cessation of stimulation. After 10 min of resting period, 1200 APs at 10 Hz were given to unload and measure the amount of loaded FM 1-43. The same neurons were stimulated again in the presence of FM 1-43 and kept in the presence of dye for an additional 30 s after stimulation to label post stimulus endocytosed vesicles. After 10 min of resting period, 1200 APs at 10 Hz were given to unload and measure the amount of loaded FM 1-43. Fully unloaded images were taken after each unloading. Net fluorescence changes were

obtained by subtracting the intensity of the unloaded image from the intensity of the loaded image.

Immunoprecipitation

HEK 293T cells transfection were carried out using Lipofectamine 2000. Cells were washed twice with cold PBS and extracted for 1 hour at 4°C in original RIPA buffer containing the following (in mM): 50 Tris HCl, pH7.5, 5 EDTA, 150 NaCl, 1% NP-40, 1 sodium orthovanadate, 1 PMSF, 10 leupeptin, 1.5 pepstatin, and 1 aprotinin. The extracts were then clarified by centrifugation at 13,000 x g for 10 min, and concentration of the protein in the supernatants was determined using bicinchoninic acid protein assay reagent kit. Samples containing 1mg of total protein were then taken for subsequent immunoprecipitation for 4 hours with anti-GFP antibody, followed by an additional 4 h of incubation at 4°C with protein G-Sepharose beads (Amersham Biosciences). The immunoprecipitates were extensively washed with the lysis buffer and then subjected to SDS-PAGE and were used for immunoblot analysis.

RESULTS

Expression pattern of SCAMP5 protein during development of neuron in hippocampal culture

To examine the expression of SCAMP5 in rat brain, cultured hippocampal neurons and SCAMP5 specific antibody were used for Western blot experiments. Figure 1 shows that SCAMP5 was expressed in hippocampal neuron, its expression levels increase during DIV 3-14 and then the level persist.

SCAMP5 shows a similar expression pattern to other synaptic vesicle proteins such as synaptotagmin1, which shows an augmented abundance with the neuronal maturation. Unlike other SCAMPs isoforms, SCAMP1 was detectable from the early embryonic phase and SCAMP5 from the postnatal development phase. On the basis of this feature of SCAMP5, one could raise a proposal on the specialized role of SCAMP5 in synapse formation and stabilization.

Suppression of SCAMP5 expression by shRNAs

To gain quantitative insight into the effect of reduced SCAMP5 expression on SV trafficking, I used two independent shRNA constructs. Suppression of SCAMP5 expression was confirmed in HEK 293T cells cotransfected with EGFP-SCAMP5 and SCAMP5-shRNA. The two shRNAs reduced SCAMP5 expression to <35 % (shRNA#1) and < 10 % (shRNA#2) of the original levels,

respectively (Figure2 A1-A2). Additionally, adeno-associated virus-mediated knockdown (KD) (shRNA#2) of endogenous SCAMP5 in neurons substantially reduced the expression of SCAMP5, while SCAMP1 and other synaptic vesicle proteins, such as synaptophysin and synaptobrevin-2, were not affected (Figure 2C). These results suggest the effect of SCAMP5 shRNA#1 and #2, specifically suppress SCAMP5, and do not affect the other synaptic vesicle protein expression.

Suppression of SCAMP5 expression resulted in a reduction of the total as well as recycling SV pool size

To gain an insight into the effect of SCAMP5 KD on presynaptic function, neurons were co-transfected with vGlut1-pHluorin (vGpH) and SCAMP5 shRNA. vGpH is a vesicular glutamate transporter-1 fused with pHluorin; a modified GFP with high pH sensitivity (43, 44). The fluorescence of which is quenched in acidic conditions and increased in basic conditions within the lumen of SVs and upon exocytosis to the extracellular space.

SV pool is made up of a recycling pool consisting of a readily releasable pool and a reserve pool and a resting pool that does not normally recycle (12). The total recycling pool is defined as the amplitude of the response to 900 action potentials (APs) at 10 Hz in the presence of bafilomycin A1(Baf), a V-type ATPase inhibitor that blocks the acidification of endocytosed SVs (42). The resting pool of vesicles refractory to stimulation is uncovered by adding NH_4Cl, which traps all of the vesicles in an alkaline state (42). The recycling

vesicle pool plays an important role for maintaining the SV release upon physiological stimulation. Thus, to test the effect of SCAMP5 KD on the synaptic vesicle pool size is crucial. For the estimation of total vesicle pool size, neurons were incubated with 50 mM NH_4Cl for 1 min. The fluorescence intensity was converted into pseudocolor and comparative analysis to the total pool size was performed. I found that SCAMP5 KD resulted in a reduction of the total pool size (mean arbitrary fluorescence intensity: 1152.09 ± 17.33 for control, 717.64 ± 10.06 for KD; Figure 3A1-A3). The absolute amplitude of the vGpH signal differs from bouton to bouton due to variations in bouton size and release probability, even in individual neurons (45, 46). In order to reduce variation of bouton size, in this experiment particularly selected similar size of bouton for analysis. When I compared the pooled average amplitude of the signal following 900 APs in the presence of *Baf* with that from similar size of control boutons, it was evident that the recycling pool size was also reduced in SCAMP5 KD neurons (Figure 3B and Figure 4A-B).

The ratio of recycling/resting pool size was significantly increased with SCAMP5 KD

In this experiment to compare recycling pool and resting pool size ratio for that is independent of presynaptic heterogeneity, the fluorescence intensity was normalized to the maximum fluorescence change after NH_4Cl treatment. I found that the recycling/resting pool ratio in SCAMP5 KD neurons was significantly increased by expanding the recycling fraction at the expense of

the resting fraction (recycling fraction: resting fraction = 61.2 ± 4.8 %: 38.8 ± 4.8 % for the control; 80.1 ± 5.7 %: 19.9 ± 5.7 % for SCAMP5 KD, Figure 5A1-A3). Overexpression of SCAMP5 did not affect the SV pool composition (Figure 5B1-B3).

Knock-down of endogenous SCAMP5 slows endocytosis after stimulation

I next tested the effect of SCAMP5 KD on exo-endocytic trafficking of SVs. I found that SCAMP5 KD slowed endocytosis after stimulation. (300 APs at 10 Hz; τ = 30.28 ± 4.51 for control, 58.96 ± 4.82 for SCAMP5 KD, Figure 6A, B). When an HA-SCAMP5 that is resistant to shRNA was introduced into SCAMP5 KD neurons, the endocytic defect was fully rescued, indicating that the decrease in the rate of endocytosis was SCAMP5 specific (τ = 31.75 ± 3.19 for SCAMP5 rescue, Figure 6A, B). This indicates that SCAMP5 KD decelerates the overall rate of vesicle fusion and decreases the endocytosis rate.

The knockdown of SCAMP5 severely impairs SV endocytosis during stimulation

To distinguish between endocytosis and exocytosis effect in SCAMP5 KD, I measured the rate of endo/exocytosis respectively. Rate of exocytosis (exocytotic rate: 0.113 ± 0.03 for the control, 0.114 ± 0.04 for SCAMP5 KD,

and 0.113 ± 0.05 for SCAMP5 rescue) and rate of endocytosis during stimulation (endocytic rate: 0.046 ± 0.02 for the control, 0.010 ± 0.04 for SCAMP5 KD, and 0.043 ± 0.03 for SCAMP5 rescue) were obtained from the linear fits to the initial 30 s of traces. The most striking effect of SCAMP5 KD was, however, on endocytic kinetics during stimulation. Because changes in fluorescence levels in the presence of *Baf* reflect pure exocytosis, where changes in the absence of *Baf* represent the balance between exocytosis and endocytosis during stimulation, the time course of endocytosis during stimulation could be estimated by simply subtracting the fluorescence values (48). I found that in control synapses, ~40% of the membrane that had undergone exocytosis had already been recovered by endocytosis during a stimulation of 300 APs at 10 Hz. In SCAMP5 KD neurons, however, <10% of the exocytosed SVs had been recovered by endocytosis during that stimulus (Figure 7A1-B3). The ratio of endocytosis/exocytosis during stimulation, calculated by obtaining the slopes after linear fitting of the time course of endocytosis and exocytosis to the 300 AP train, was significantly reduced in SCAMP5 KD neurons compared to controls (Figure 7B4), pointing to severe endocytic defects in these neurons. Again, the endocytic defects were fully rescued in neurons containing HA-SCAMP5 resistant to shRNA (Figure 7A3 and B4).

SCAMP5 Knock down caused by independent shRNA#1 (SCAMP5-specific shRNA was designed from the rat SCAMP5 cDNA sequence targeting to the region of nucleotides 54-74), the ratio of endocytosis/exocytosis during stimulation (300APs 10Hz), was also remarkably reduced in SCAMP5 KD

neurons compared to controls (endo/exo ratio 0.386 ± 0.06, n = 8 for control, 0.097 ± 0.05, n = 10 for SCAMP5 KD; Figure 8A1-B1).

Thus, SCAMP5 is required for the endocytosis during stimulation as well as after stimulation, to efficiently persistent in the synaptic vesicle recycling process.

The average time courses of endocytosis clearly revealed severe defects in endocytosis during stimulation by SCAMP5 KD

The endocytic defects observed during stimulation of SCAMP5 KD neurons became more evident when the average time courses of exocytosis and endocytosis in control and SCAMP5 KD neurons were compared. There was no statistically significant difference between the average time course of exocytosis from control and SCAMP5 KD neurons (exocytotic rate: 0.113 ± 0.03 for the control, 0.114 ± 0.04 for SCAMP5 KD, and 0.113 ± 0.05 for SCAMP5 rescue; endocytic rate: 0.046 ± 0.02 for the control, 0.010 ± 0.04 for SCAMP5 KD, and 0.043 ± 0.03 for SCAMP5 rescue); indicating that the kinetics of SV exocytosis were not affected by SCAMP5 KD and that SCAMP5 functions in the endocytic pathway (Figure 9A). A composite graph of the average time course of total endocytosis was obtained by combining the time course of endocytosis during stimulation (i.e. (+)*Baf* – (-)*Baf*) with the inverse image of the time course of endocytosis after stimulation (Figure 7A1-A3). Compared with control and SCAMP5 KD-rescued neurons (Figure 9A

black and blue lines, respectively), SCAMP5 KD neurons (Figure 9A, red line) showed considerable defects in endocytosis during stimulation, whereas post-stimulus endocytosis was only mildly affected (Figure 9A). With prolonged stimulation (900 APs at 10 Hz), the endocytic defects in SCAMP5 KD synapses during stimulation were more pronounced than in the control synapses and virtually no exocytosed SVs were endocytosed (Figure 9B). Therefore, these results further demonstrate that SCAMP5 importantly involved in controlling the endocytosis during strong stimulation to maintain sustained synaptic transmission.

Independent verification of SCAMP5 KD-induced endocytic defects during stimulation using synaptophysin-pHluorin.

To avoid a possible bias caused by an SV protein-specific recycling mode (49, 50), SypHy, a fusion protein of synaptophysin with pHluorin, was used (51). In agreement with the data obtained from vGpH-transfected neurons, SV endocytosis during stimulation was again severely defective in the SCAMP5 KD neurons and was fully rescued by the expression of HA-SCAMP5 resistant to shRNA (Figure 10A-D), indicating that the SV retrieval defect caused by SCAMP5 KD is independent of the particular SV protein used.

Independent verification of SCAMP5 KD induced endocytic defects during stimulation using FM 1-43

To further eliminate any influence of an SV protein-specific endocytic mode on the analysis, FM1–43, green fluorescent strylyl membrane dye that is widely used to study SV recycling kinetics (52, 53), was used. I used FM1-43 uptake experiment to test whether SV recycling was altered by SCAMP5 KD (Figure 11A). In first loaded of FM 1-43 dye, control and SCAMP5 KD neurons were exposed to the FM1-43, and stimulated 30 sec at 10 Hz then washed for 10 min. Next, the neurons are stimulated with 1,200APs at 10 Hz to drive maximal dye release from synaptic vesicles. In second loaded of FM 1-43, neurons exposed to the FM 1-43 until 30 sec after stimulation, then washed for 10 min. When FM 1-43 was present during stimulation of SCAMP5 KD neurons, the amount of endocytosed FM 1-43 was considerably lower than that of control (20.45 ± 0.05% for the control), but after continued incubation with FM 1-43 after stimulation, the difference was substantially reduced (66.36 ± 0.01% for the control), again indicating that the severe endocytic defect observed in the period of stimulation (Figure 11B1-B4) These results consistent with the endocytic defect observed using pHluorin (vGpH, SypHy), suggesting that SCAMP5 is essential for the endocytic process.

Synaptic vesicle re-acidification was not affected by SCAMP5 KD

To confirm the endocytosis defect occurred during stimulation was not due to the deficient of SV re-acidification in SCAMP5 KD neurons, I compared the re-acidification kinetics between control and SCAMP5 KD The extracellular solution is changed twice from pH 7.7 to 5.5 back and after a 30 sec stimulus, fluorescence was quenched to the same extent level as the pre-stimulus period (average degree of quenching post-stimulus: 94.11 ± 5.88% in control and 95.11 ± 4.88% in SCAMP5 KD; Figure 12A1-B2). These experiment suggest that the synaptic vesicle re-acidification was unaffected by SCAMP5 KD.

The knockdown of SCAMP5 lowers the threshold of activity at which the SV endocytosis becomes unable to compensate for ongoing the exocytosis during the stimulus

Next, I plotted endocytosis/exocytosis ratios during stimulation of 300 APs at different frequencies. I found that, at the lower stimulation frequency, 5 Hz , SCAMP5 KD synapses did not show a significant endocytic defect (endocytosis/exocytosis ratio: 0.790 ± 0.032 for control, 0.747 ± 0.054 for SCAMP5 KD), indicating that SCAMP5 KD synapses performed endocytosis normally when the exocytosis burden was low (Figure 13A1-A3). At 10 Hz, however, SCAMP5 KD synapses displayed severe endocytic defects during

stimulation (endocytosis/exocytosis ratio: 0.091 ± 0.032; for control, 0.421 ± 0.07 for SCAMP5 KD). At a higher stimulation frequency of 20 Hz, the endocytosis/exocytosis ratio in control synapses was also dramatically decreased, suggesting that the cell's endocytic capacity was saturated with an increased stimulus frequency of 20 Hz (Figure 13A1 and A4-A5). The inability of SCAMP5 KD neurons to match the rate of endocytosis to that of the ongoing exocytosis at 10 Hz was corroborated by the finding that when extracellular [Ca^{2+}] was decreased to 0.75 mM to reduce the SV release probability (i.e. to reduce the exocytotic load) (45, 46), the endocytic defects of the SCAMP5 KD synapses were less severe at 10 Hz (endocytosis/exocytosis ratio: 0.436 ± 0.007 at 0.75 mM [Ca^{2+}]; Figure 13B).

The frequency, not the duration, of stimulation is important for the observed defects in endocytosis in SCAMP5 KD

The endocytic defects of SCAMP5 KD synapses at 10 Hz were also observed with 15 s stimulation (150 APs; Figure 14A1-A3 and D). With a 10 s stimulation at 20 Hz (200 APs), I again found that endocytic capacity was saturated in the control (Figure 14B1-B3), as in the case with 30 s stimulation at 20 Hz (600 APs) (Figure 14C1-C3 and E), suggesting that the frequency of stimulation (i.e. how fast exocytosis occurs so that how fast SVs accumulate on the plasma membrane over the endocytic capacity) is important. These results indicate that KD of SCAMP5 lowers the threshold of synaptic activity

at which SV endocytosis becomes unable to compensate for ongoing exocytosis during stimulation.

The ratio of the recycling/resting pool size was significantly increased with SCAMP5-Nterm overexpression

To determine which domain of SCAMP5 is involved in the changes of recycling/resting SV pool ratio, I focused on the cytoplasmic regions (N-term, 2/3 loop and C-term) of the SCAMP5 domain. Neurons were overexpressed with SCAMP5 N-term, 2/3loop, or C-term, respectively. The results showed that Nterm overexpression expanded the proportion of the recycling pool size (0.57 ± 0.08 : 0.42 ± 0.08 for the control, 0.69 ± 0.04 : 0.31 ± 0.04 for the SCAMP-Nterm overexpression) (Figure 16 A1-A2 and B1). The opposite effect was noted for the 2/3loop overexpression: the recycling pool fraction was reduced, and the C-term overexpressed neurons showed no changes in pool size fraction (0.36 ± 0.04 : 0.63 ± 0.04 for the SCAMP5-2/3loop; 0.56 ± 0.05 : 0.43 ± 0.05 for the SCAMP-Cterm) (Figure 16 A3-A4 and B2). Therefore, the N-term and 2/3loop domain of SCAMP5 are related to modulation of the SV pool size.

Overexpression of SCAMP5-Nterm induced impairment of SV endocytosis during stimulation

Since the N-term of SCAMP5 showed a comparable change to SCAMP5 KD in SV pool ratio, I tested whether SCAMP5 N-term cytoplasmic tail is responsible for the endocytic defects found in SCAMP5 KD synapse. I first found that SCAMP5 N-term cytoplasmic tail contains putative AP-2 binding sites, YXXϕ. The μ subunit of AP-2 is known to bind the sorting signal motif YXXϕ (where ϕ is a bulky hydrophobic residue) of the cargo molecules (54-56). To test the effect of the N-terminal region of SCAMP5 in SV recycling, I transfected hippocampal neurons with mCherryC1, mCherry-SCAMP5 Nterm, mCherry-SCAMP5 Nterm (m) (SCAMP5 Nterm tyrosine 22 to alanine point mutant) to analyze the SV retrieval. I found that SCAMP5 Nterm expression caused the defect of endocytosis during stimulation (exocytotic rate: 0.132 ± 0.04 for the control, 0.143 ± 0.05 for SCAMP5 N-term, 0.139 ± 0.06 for SCAMP5 N-term mutant; endocytic rate: 0.052 ± 0.04 for the control, 0.020 ± 0.04 for SCAMP5 N-term, 0.057 ± 0.05 for SCAMP5 N-term mutant). The Nterm (Y22A) point mutant, however, showed no defects in endocytosis during stimulation (Figure 17 A1-B3 and C). These results showed that the N-terminal domain of SCAMP5 that contain AP-2 binding motif is responsible for endocytosis during neuronal activity.

The 2/3loop domain of SCAMP5 had no effect on the SV endocytosis during sustained stimulation

I found that 2/3loop overexpression led to a reduction in the ratio of recycling/resting pool size. Besides, I found that 2/3loop also contains an AP-2 binding motif (YXXϕ). Unlike the effect of N-term, however, the results showed that the 2/3loop has no effect on SV endocytosis (exocytotic rate: 0.133 ± 0.05 for the control, 0.118 ± 0.06 for SCAMP5-2/3loop; endocytic rate: 0.052 ± 0.04 for the control, 0.045 ± 0.05 for SCAMP5-2/3loop) (Figure 18A1-C). Thus, I concluded that 2/3loop region is not a major requirement for endocytosis and that the N-terminal region of SCAMP5 is more important for SV retrieval during sustained neuronal stimulation.

SCAMP5 binds to AP-2 through its N-terminal domain.

I already mentioned that SCAMP5 contains two putative AP-2 binding sites (YXXϕ) in the N-terminal and 2/3loop region. Since the results from the overexpression of SCAMP5 N-term resemble what I found with SCAMP KD, I assessed whether SCAMP5 indeed physically interacts with AP-2 via its N-term. HEK 293 cells were transfected with GFP-SCAMP5, GFP-SCAMP5 Nterm or GFP-SCAMP5 Cterm and immunoprecipitated with anti-GFP antibody (Figure 19). Immunoblot analysis with the anti-AP-2 antibody showed that SCAMP5 and the SCAMP5 N-terminal directly interact with AP-

2. These results show that SCAMP5 binds to AP-2 through its N- terminal domain.

The recruitment of SVs for release during multiple stimuli was reduced in SCAMP5 KD

To test SVs's consumption during sustained stimulation, neurons were co-transfected with the pU6mRFP-vector and vGpH (control) or SCAMP5 shRNA and vGpH (SC5 KD). I used *Baf*, so when the SVs containing vGpH were trapped in the alkaline state and hence fluoresced after vesicle exocytosis. The fluorescence accumulation was elicited by successive 10 trials of 20 Hz stimulation. In SCAMP5 KD, the accumulative response of the trials was significantly reduced compared with the control (29.79% ± 7.2% for the control; 11.64% ± 4.3% for SCAMP5 KD, n=5 for each) (Figure 20A-B).

Spontaneous neurotransmission was not affected by SCAMP5 KD

In resting state, neurotransmitters are released without action potentials (this is known as spontaneous release) primarily in a Ca^{2+} dependent manner (57, 71, 72). Recently, evidence has suggested that the Vps10p-tail-interactor-1a (Vti1a) -containing SVs are mainly mobilized in the resting state, but not during neuronal activity and that Vti1a selectively maintains spontaneous neurotransmitter release (50), leading to conclusion that SVs related to

spontaneous neurotransmission are distinct from the evoked release. To test the SCAMP5 effects on the spontaneous neurotransmitter release, I measured spontaneous and evoked release in different calcium concentrations (0.75mM, 2mM, and 4mM) (Figure 21 A1-C2). The results showed that spontaneous neurotransmission is not affected by SCAMP5 KD.

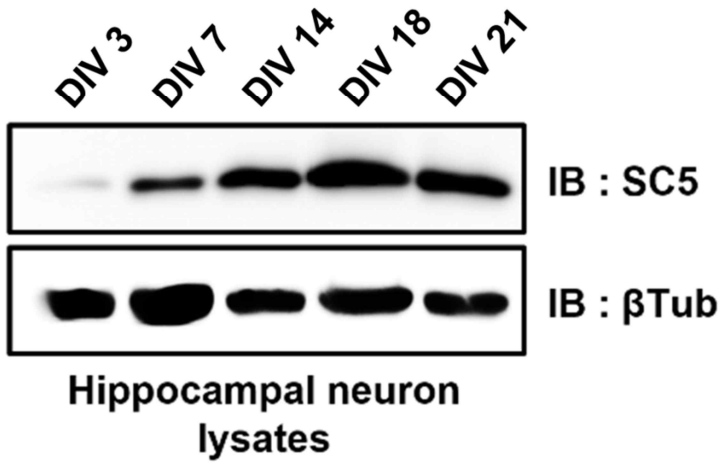

Figure 1. Developmental changes of SCAMP5 protein expression in cultured rat hippocampal neurons.

Cultured primary hippocampal neurons were prepared at the indicated days in vitro (DIV), lysed, and evenly loaded (75 μg) in SDS- PAGE gel. Western blot analysis was performed using a specific anti-SCAMP5 antibody. SC5:SCAMP5, βTub: β-tubulin. SCAMP5 expression rises during DIV 3 to 14 and then the levels persisted.

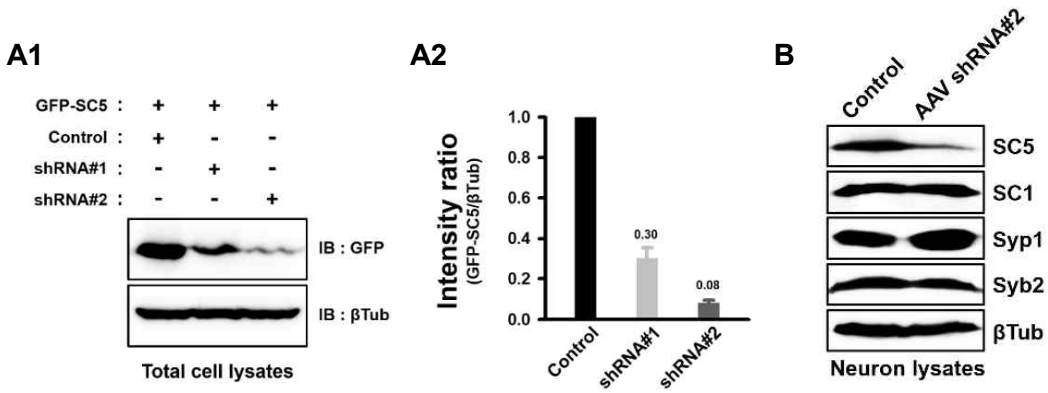

Figure 2. Suppression of SCAMP5 expression by shRNAs.

A1-2, HEK293T cells were co-transfected with EGFP-SCAMP5 and pU6mRFP-vector (control) or pU6mRFP-SCAMP5-specific shRNAs, respectively. 72 h after transfection, the cells were lysed, and evenly loaded (25 μg) in SDS-PAGE. Western blot analysis was performed using anti-GFP antibody and anti-βTub antibody. Both SCAMP5-targeted shRNAs efficiently knocked-down the expression of GFP-SCAMP5 (expression levels over control: 0.3 ± 0.04 for shRNA#1, n = 4, 0.08 ± 0.01 for shRNA#2, n = 4). **B,** Immunoblot analysis of primary cultured neurons infected with control or SCAMP5 shRNA#2-based adeno-associated virus (SC5 shRNA#2) for endogenous SCAMP5 knockdown. The cells were infected at DIV 7 and were lysed at DIV 21. Western blot analysis was performed using indicated specific antibodies. SC1: SCAMP1; Syp1: synaptophysin 1; Syb2: synaptobrevin 2; βTub: β-Tubulin.

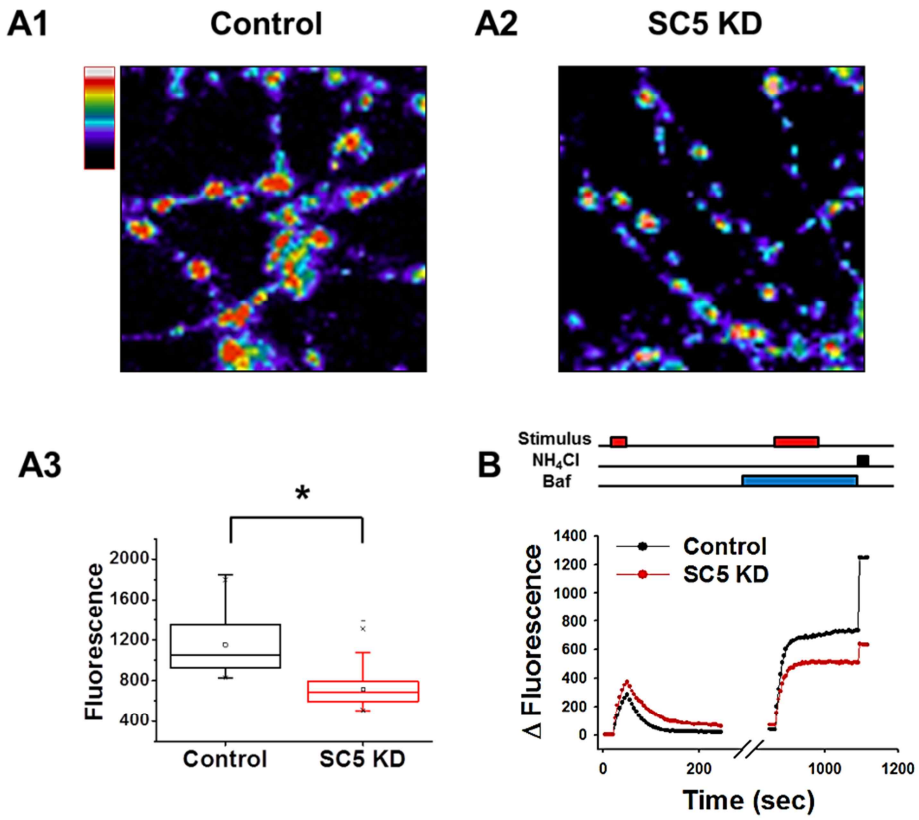

Figure 3 Suppression of SCAMP5 expression resulted in a reduction of total as well as recycling SV pool size

A1-2, Representative fluorescence images of control and KD neurons transfected with vGpH, and treated with NH_4Cl to reveal total vesicle pool size of given boutons. Pseudo-color indicates relative fluorescence intensities. **A3,** a box-and-whiskers graph of total vesicle pool size (median: 1054.098 and 682.936; upper and lower quartiles: upper 1347.681 and 792.491, lower 925.049 and 596.255; maximum values: 1843.495 and 1385.644; minimum values: 828.552 and 502.826 for control and SCAMP5 KD, respectively.

Open circle indicates mean: 1152.09 ± 17.33, n = 5 for control, 717.64 ± 10.06, n = 6 for KD. **B,** Representative pooled average vGpH profiles for comparison of recycling pool size and total vesicle pool size between control and SCAMP5 KD synapses. Neurons were stimulated with 300 APs at 10 Hz without *Baf*. After 10 min resting period, neurons were stimulated with 900 APs at 10 Hz in the presence of *Baf*. The change in fluorescence intensity to the plateau reflects the entire recycling pool. All remaining acidic vesicles are alkalized by NH_4Cl treatment, revealing the size of the resting pool. Due to variation in bouton size even in an individual neuron, we choose to compare the similar size of boutons from control and KD neurons (n = 25 for control and 25 for KD)

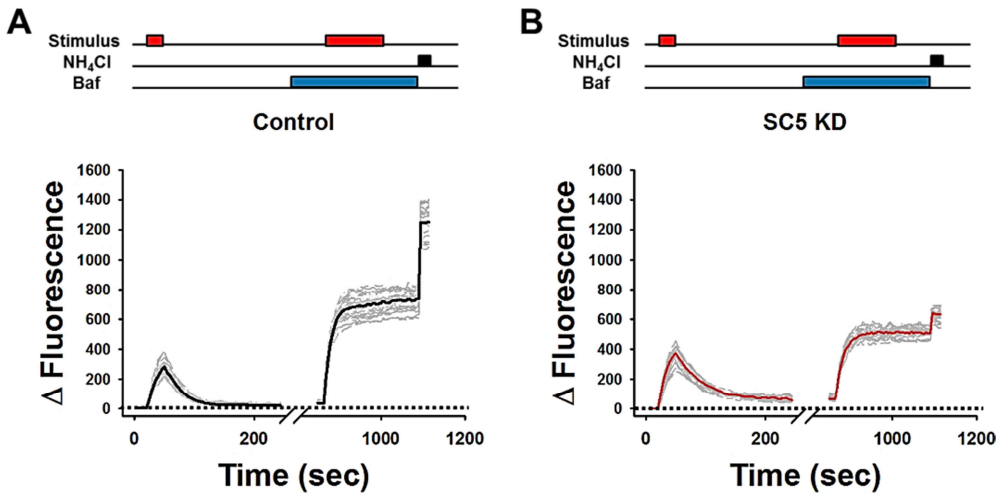

Figure 4. In synaptic vesicle pool size measurement, non-normalized fluorescence changes were reduced in SCAMP5 KD.

The representative experiment used to measure non-normalized fluorescence changes to showing the total synaptic vesicle pool and recycling pool size. The fluorescence changed response of vGpH transfected neurons. (n = 25 for control and 25 for KD). Neurons were stimulated with 300 APs at 10 Hz without *Baf*. After 10 min resting periods, the same neurons were stimulated with 900 APs at 10 Hz in the presence of *Baf*. NH4Cl application induced a further increase in fluorescence, reflects the entire resting vesicle pool. In figure 1-3B expressed averaged value of the fluorescence change were from common data used in Figure 1-4 A and B.

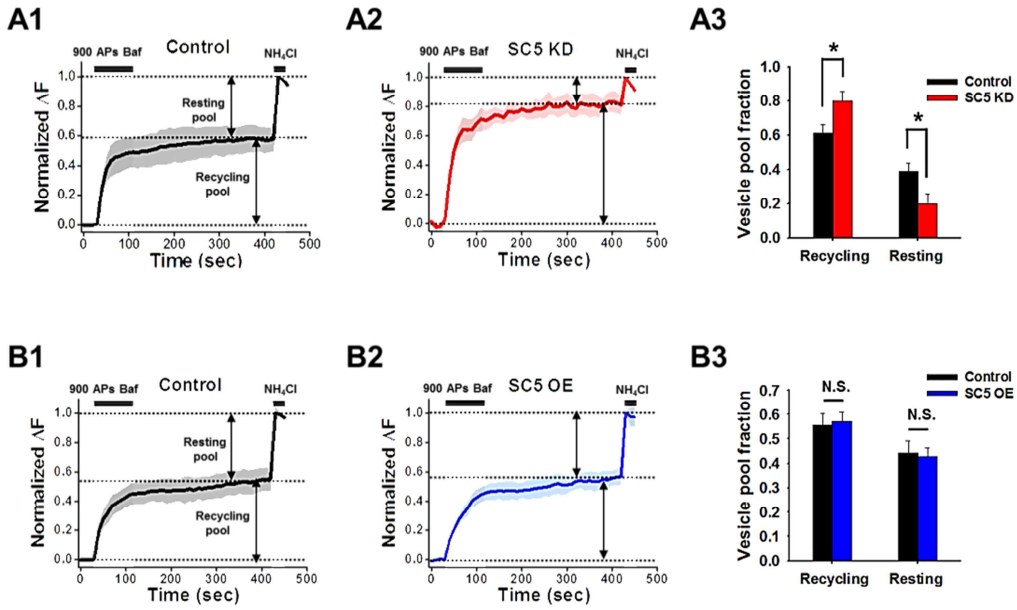

Figure 5. The ratio of recycling/resting pool size was significantly increased in SCAMP5 KD.

A1-A2, Averaged time course of vGpH fluorescence traces in the presence of *Baf* followed by NH_4Cl treatment. The absolute amplitude of the signal differs from bouton to bouton due to variation in vesicle pool size even in an individual neuron, so I normalized the each pool size to the total vesicle pool size (i.e. to the maximum fluorescence change after NH_4Cl treatment), providing a signal that is independent of vesicle pool size.(n = 12 for control, 14 for KD) **A3,** Average fraction values of recycling : resting pool for control,

and SCAMP5 KD synapses (0.61 ± 0.04 : 0.39 ± 0.04 for control *vs.* 0.80 ± 0.05 : 0.19 ± 0.05 for KD). Data are presented as means ± s.e. * $p < 0.01$ (Student's *t*-test). **B1-B2,** Averaged time course of vGpH fluorescence traces in control and SCAMP5 overexpressed synapses (n = 11 for control, 13 for OE) **B3,** Average fraction values of recycling : resting pool for control, and SCAMP5- overexpressed synapses (0.56 ± 0.04 : 0.44 ± 0.04 for control *vs.* 0.58 ± 0.03 : 0.42 ± 0.03 for OE). Data are presented as means ± s.e. * $p < 0.01$ (Student's *t*-test).

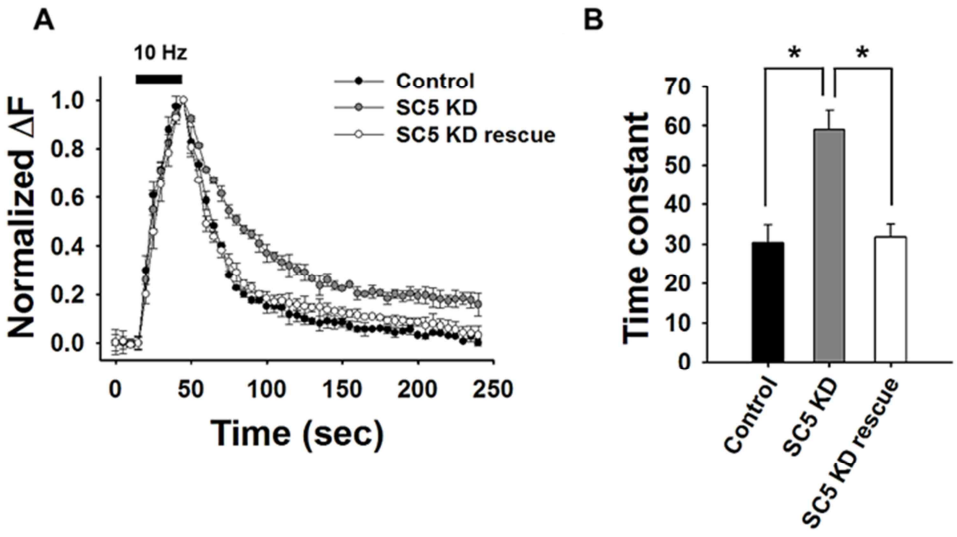

Figure 6. Knock-down of endogenous SCAMP5 slowed endocytosis after stimulation.

A, Average vGpH fluorescence intensity profiles, was plotted as $\Delta F/F_0$ against time, following stimulation with 300 APs at 10 Hz (dark bar*)*. Fluorescence values were normalized to the maximal fluorescence signal in each experimental condition. **B,** The decay of vGpH after stimulation fitted by a single exponential with time constant, $\tau = 30.28 \pm 4.51$ s for control (n = 8), 58.96 ± 4.82 s for SCAMP5 KD (n = 9), 31.75 ± 3.19 s for SCAMP5 KD rescue (n = 9). Data are presented as means ± s.e. * $p < 0.01$ (ANOVA and Turkey's HSD *post hoc* test).

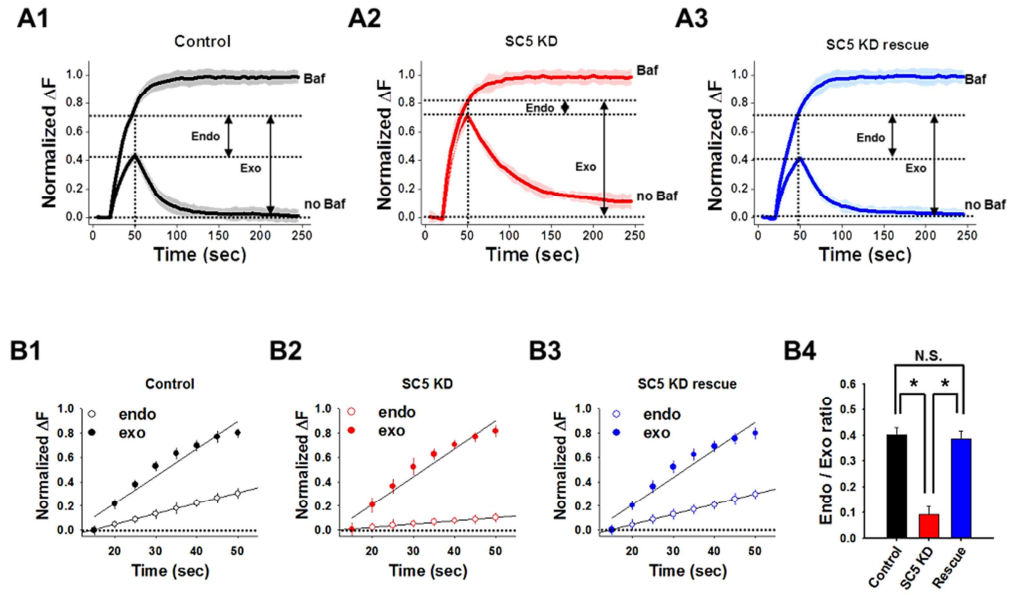

Figure 7. The knockdown of SCAMP5 severely impairs SV endocytosis during stimulation.

A1-3, Average vGpH fluorescence intensity profiles from control (A1), KD (A2), and rescued (A3) synapses stimulated with or without *Baf*. Neurons were stimulated with 300 APs at 10 Hz without *Baf*. After 10 min resting period, the same neurons were stimulated again with 1,200 APs at 10 Hz in the presence of *Baf*. Fluorescence values were normalized to the maximal stable fluorescence signal in the *Baf* trace (n = 15 for control, 15 for KD, 15 for rescue). **B1-3,** Graphs showing the time course of endocytosis (Endo) and exocytosis (Exo) during stimulation with 300 APs at 10 Hz. Time course of endocytosis during stimulation were derived by subtracting the fluorescence

trace in the absence of *Baf* ($\Delta F_{exo-endo}$) from the trace in its presence ($\Delta F_{endo} = \Delta F_{exo} - \Delta F_{exo-endo}$). Rate of exocytosis and rate of endocytosis during stimulation were obtained from the linear fits to the initial 30 s of traces (exocytic rate: 0.113 ± 0.03 for the control, 0.114 ± 0.04 for SCAMP5 KD, and 0.113 ± 0.05 for SCAMP5 rescue; endocytic rate: 0.046 ± 0.02 for the control, 0.010 ± 0.04 for SCAMP5 KD, and 0.043 ± 0.03 for SCAMP5 rescue). **B4,** Ratios of endocytosis/exocytosis rate: 0.402 ± 0.03 for the control, 0.092 ± 0.04 for SCAMP5 KD, and 0.386 ± 0.03 for SCAMP5 rescue. Data are presented as means ± s.e. * $p < 0.01$ (ANOVA and Tukey's HSD *post hoc* test).

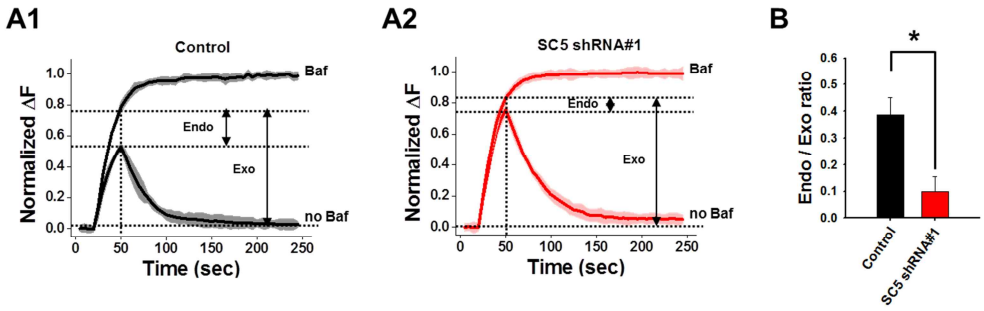

Figure 8. Endogenous SCAMP5 was knocked down by shRNA#1, which impaired endocytosis during stimulation.

A1-2, SCAMP5 KD by another independent shRNA (shRNA#1 in Figure 1-1) also resulted in a severe defect in the endocytosis during stimulation. **B,** The average endo/exo ratio (0.386 ± 0.06, n = 8 for the control, 0.097 ± 0.05, n = 10 for SCAMP5 KD) during 300 APs at 10 Hz. Data are presented as means ± s.e. * $p < 0.01$ (ANOVA and Turkey's HSD *post hoc* test).

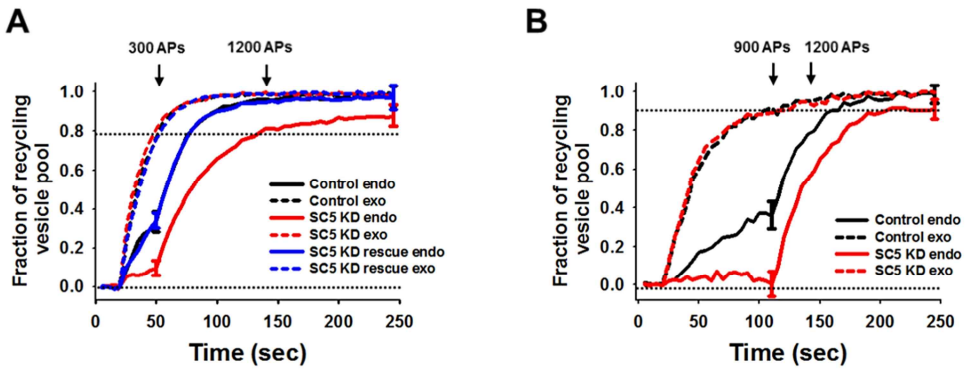

Figure 9. Average time courses of endocytosis clearly revealed severe defects in endocytosis during stimulation by SCAMP5 KD.

A, Average time course of endocytosis from control (black), KD (35), and rescue (blue) neurons during and after 300 APs at 10 Hz without *Baf* and the average time course of exocytosis from control (black dotted), KD (red dotted), and rescue (blue dotted) neurons during 1,200 APs at 10 Hz with *Baf*. A composite graph of the average time course of total endocytosis was obtained by combining the time course of endocytosis during stimulation (i.e. (+)*Baf* – (-)*Baf*) with the inverse image of the time course of endocytosis after stimulation in Figure 1-4A1-A3. The dashed line indicates the extent of exocytosis at the 30 s time point where the endocytosis to exocytosis ratios is calculated. Error bars at two time points on the endocytosis curves. **B,** Average time course of endocytosis from control (black), KD (35) neurons during and after 900 APs at 10 Hz without *Baf* and the average time course of exocytosis from control (black dotted), KD (red dotted) neurons during 1,200 APs at 10 Hz with *Baf*. Error bars at two time points on the endocytosis curves.

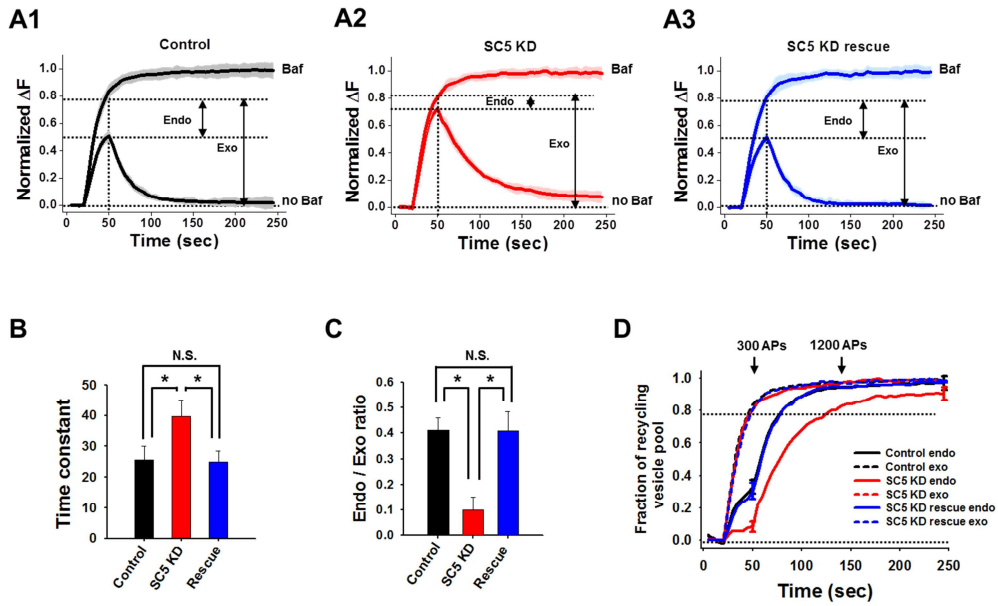

Figure 10. Independent verification of SCAMP5 KD induced endocytic defects during stimulation using synaptophysin-pHluorin

A1-3, Average SypHy fluorescence intensity profiles from control (A1), KD (A2), and rescued (A3) synapses stimulated with or without *Baf*. Neurons were stimulated with 300 APs at 10 Hz without *Baf*. After 10 min resting period, the same neurons were stimulated again with 1,200 APs at 10 Hz in the presence of *Baf*. Fluorescence values were normalized to the maximal stable fluorescence signal in the *Baf* trace**. B,** Decay of SypHy after stimulation fitted by a single exponential with time constant, τ =25.66 ± 4.51 s for control (n = 8), 39.59 ± 5.53 s for SCAMP5 KD (n = 10), 24.87 ± 6.13 s

for SCAMP5 KD rescue (n = 8). Data are presented as means ± s.e. * $p < 0.01$ (ANOVA and Turkey's HSD *post hoc* test). **C,** Rate of exocytosis and rate of endocytosis during stimulation were obtained from the linear fits to the initial 30 s of traces (exocytic rate: 0.134 ± 0.04 for the control, 0.133 ± 0.04 for SCAMP5 KD, and 0.131 ± 0.06 for SCAMP5 rescue; endocytic rate: 0.055 ± 0.03 for the control, 0.0135 ± 0.04 for SCAMP5 KD, and 0.053 ± 0.04 for SCAMP5 rescue). The ratios of endocytosis/exocytosis rate: 0.410 ± 0.04 for the control, 0.101 ± 0.05 for SCAMP5 KD, and 0.408 ± 0.07 for SCAMP5 rescue. Data are presented as means ± s.e. * $p < 0.01$ (ANOVA and Tukey's HSD *post hoc* test). **D,** The average time course of endocytosis from control (black), KD (35), and rescue (blue) neurons during and after 300 APs at 10 Hz without *Baf* and the average time course of exocytosis from control (black dotted), KD (red dotted), and rescue (blue dotted) neurons during 1,200 APs at 10 Hz with *Baf*. The dashed line indicates the extent of exocytosis at the 30 s time point where the endocytosis to exocytosis ratios is calculated. Error bars at two time points on the endocytosis curves.

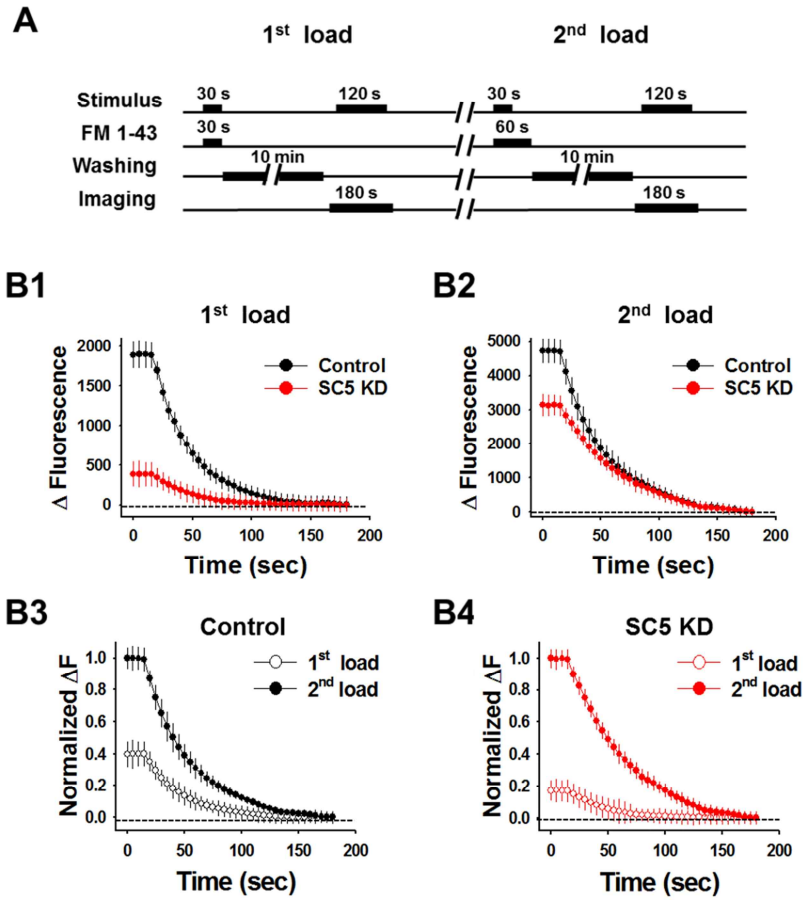

Figure 11. Independent verification of SCAMP5 KD induced endocytic defects using FM 1-43.

A, Experimental protocol used to compare endocytosis during stimulation and after stimulation using FM 1-43. For endocytosis during stimulation, FM 1–43 was loaded with the onset of stimulation (300 APs) and immediately washed out with the cessation of stimulation. After 10 min of resting period,

1,200 APs at 10 Hz were given to unload and measure the amount of loaded FM 1-43. The same neurons were stimulated again in the presence of FM 1-43 and kept in the presence of dye for an additional 30 s after stimulation to label post-stimulus endocytosed vesicles. After 10 min of resting period, 1,200 APs at 10 Hz were given to unload and measure the amount of loaded FM 1-43. **B1-2,** The pooled average traces of FM 1-43 signal of 1^{st} load(F1) or 2^{nd} load(F2) from the similar size of boutons in control (black) and SCAMP5 KD (35) during 1,200 APs stimulation (F1 : 1894.33 ± 169.97, n = 8 for control, 387.54 ± 160.83, n = 10 for KD; F2 : 4723.83 ± 366.68 for control, 3135 ± 328.78 for KD). **B3-4**, The normalized average time course of FM 1-43 fluorescence intensity of 1^{st} and 2^{nd} load during unloading with 1,200 APs at 10 Hz. Fluorescence values were normalized to the maximal FM 1-43 fluorescence signal after 2^{nd} load (1^{st} load over 2^{nd} load : 0.401 ± 0.082 for control, 0.173 ± 0.039 for KD).

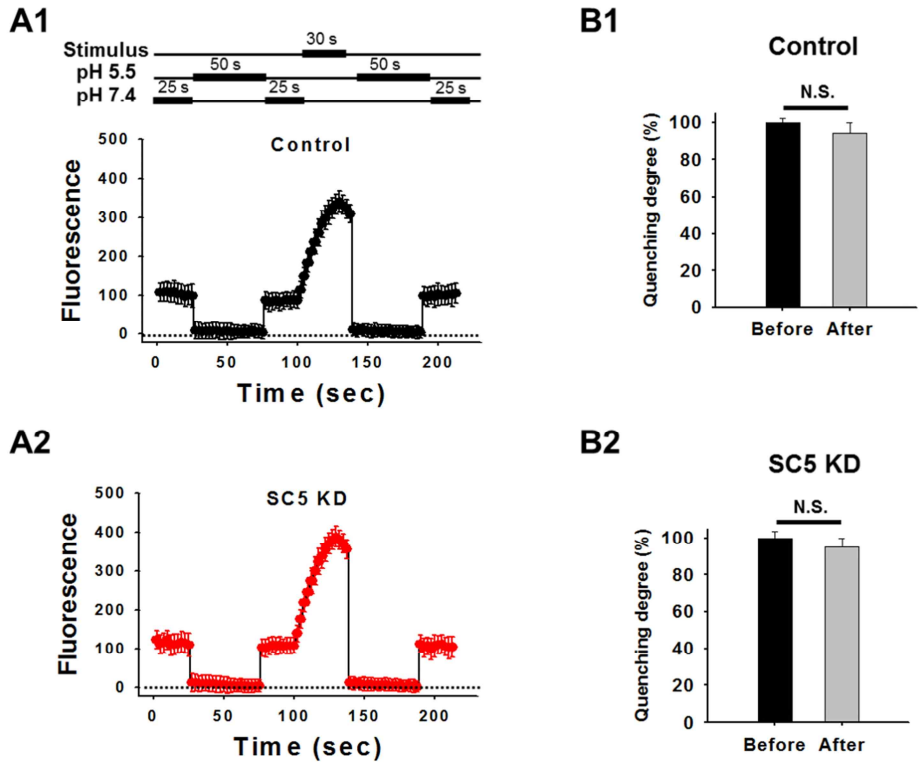

Figure 12. Synaptic vesicle re-acidification was not affected by SCAMP5 KD

A1-2, Average races of synaptopHluorin signal in control and SCAMP5 KD during pH exchange experiments. The extracellular solution is changed twice from pH 7.4 to 5.5 and back. Extracellular application of pH 5.5 Tyrode solution rapidly quenches all surface sPH in the pre-stimulus period. After 50 s, the extracellular solution is changed back to pH 7.4. Following a 30 s stimulus at 10 Hz, the extracellular solution is changed to pH 5.5 for 50 s then back to pH 7.4. Net sPH fluorescence changes were obtained by subtracting the average intensity of the first pH 5.5 challenge ($F_{5.5}$) from the intensity of

each frame (F_t) for individual boutons and averaged.**B1-B2,** Average degree of quenching post-stimulus was 94.11 ± 5.88% in control (n = 5) and 95.11 ± 4.88% in KD (n = 6).

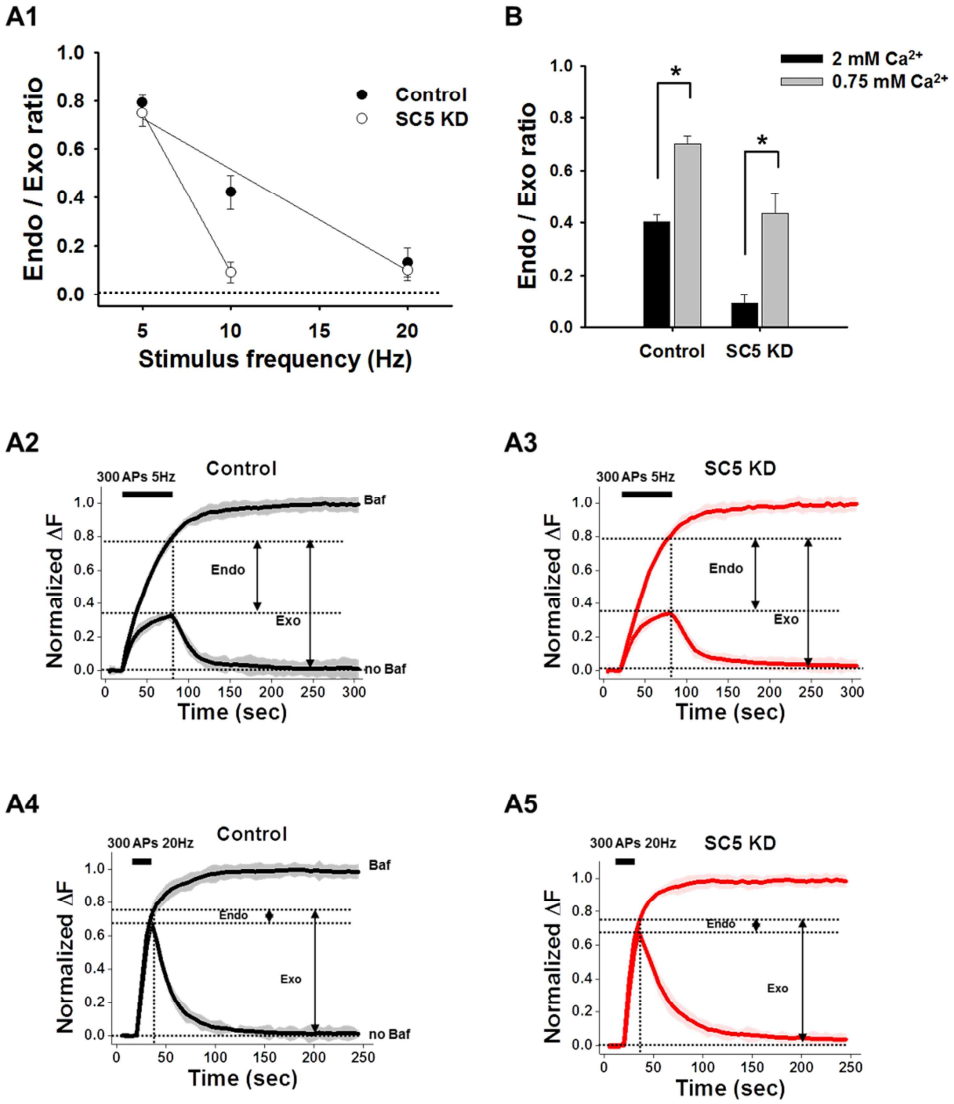

Figure 13. Knockdown of SCAMP5 lowers the threshold of activity at which the SV endocytosis becomes unable to compensate for ongoing the exocytosis during the stimulus.

A1, Endo/exo ratios after 300 APs at different frequencies. Dashed lines are linear-fits (control: KD = 0.790 ± 0.03 : 0.751 ± 0.05 at 5 Hz, 0.421 ± 0.07 : 0.091 ± 0.04 at 10 Hz, 0.131 ± 0.06 : 0.099 ± 0.03 at 20 Hz). n = 8 for control,

n = 8 for KD at each frequency. **A2-A5**, Average vGpH fluorescence intensity profiles from control, SC5 KD stimulated with 300 APs 5 Hz (A2-A3) and 300APs 20Hz (A4-A5). **B,** Mean endo/exo ratios after 300 APs at 10 Hz in 2 mM or 0.75 mM extracellular [Ca^{2+}]. At 0.75 mM [Ca^{2+}], Endo/Exo ratio: 0.701 ± 0.03, n = 5 for control, 0.436 ± 0.01, n = 7 for KD. Data are presented as means ± s.e. * $p < 0.01$ (Student's *t*-test).

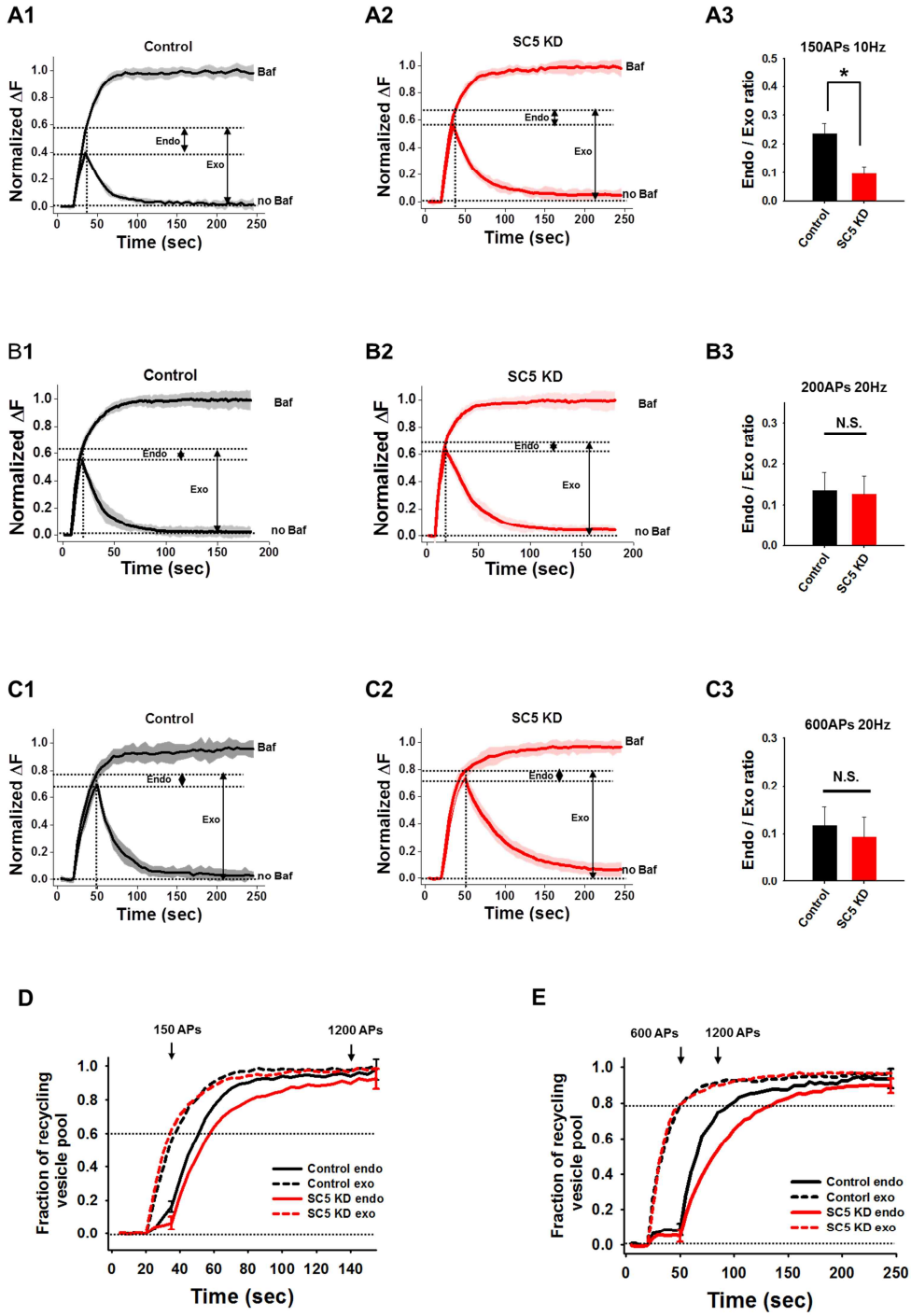
A1
Control
Normalized ΔF
Baf
Endo
Exo
no Baf
Time (sec)
A2
SC5 KD
A3
150APs 10Hz
Endo / Exo ratio
Control
SC5 KD
B1
B2
B3
200APs 20Hz
N.S.
C1
C2
C3
600APs 20Hz
D
150 APs
1200 APs
Fraction of recycling vesicle pool
Control endo
Control exo
SC5 KD endo
SC5 KD exo
E
600 APs
1200 APs

Figure 14. The frequency, not the duration, of stimulation was important for the observed defects in endocytosis in SCAMP5 KD.

A1-2, Average vGpH fluorescence intensity profiles from control (A1), and KD (A2) synapses stimulated with or without *Baf*. Neurons were stimulated at 10 Hz for 15 s (150 APs) without *Baf*. After 10 min resting period, the same neurons were stimulated again with 1,200 APs at 10 Hz in the presence of *Baf*. Fluorescence values were normalized to the maximal stable fluorescence signal in the *Baf* trace (n = 9 for control, n = 10 for SCAMP5 KD). **A3**, Ratios of endocytosis/exocytosis rate: 0.236 ± 0.04 for control, 0.096 ± 0.03 for SCAMP5 KD. **B1-2,** Average vGpH fluorescence intensity profiles from control (B1), and KD (B2) synapses stimulated with or without *Baf*. Neurons were stimulated at 20 Hz for 10 s (200 APs) without *Baf*. After 10 min resting period, the same neurons were stimulated again with 1,200 APs at 20 Hz in the presence of *Baf*. Fluorescence values were normalized to the maximal stable fluorescence signal in the *Baf* trace (n = 10 for control, n = 11 for SCAMP5 KD) **B3,** Ratios of endocytosis/exocytosis rate: 0.134 ± 0.04 for control, 0.127 ± 0.05 for SCAMP5 KD. **C1-2,** Average vGpH fluorescence intensity profiles from control (C1), and KD (C2) synapses stimulated with or without *Baf*. Neurons were stimulated at 20 Hz for 30 s (600 APs) without *Baf*. After 10 min resting period, the same neurons were stimulated again with 1,200 APs at 20 Hz in the presence of *Baf*. Fluorescence values were normalized to the maximal stable fluorescence signal in the *Baf* trace (n = 11 for control, n = 11 for SCAMP5 KD). **C3,** Ratios of endocytosis/exocytosis rate: 0.116 ± 0.04 for control, 0.093 ± 0.04 for SCAMP5 KD. **D**, The average

time course of endocytosis from control (black) and SCAMP5 KD (red) neurons during and after 150 APs at 10 Hz without *Baf* and the average time course of exocytosis from control (black dotted) and SCAMP5 KD (red dotted) during 1,200 APs at 10 Hz with *Baf*. Error bars at two time points on the endocytosis curves. **E,** Average time course of endocytosis from control (black) and SCAMP5 KD (red) neurons during and after 600 APs at 20 Hz without *Baf* and the average time course of exocytosis from control (black dotted) and SCAMP5 KD (red dotted) during 1,200 APs at 20 Hz with *Baf*.

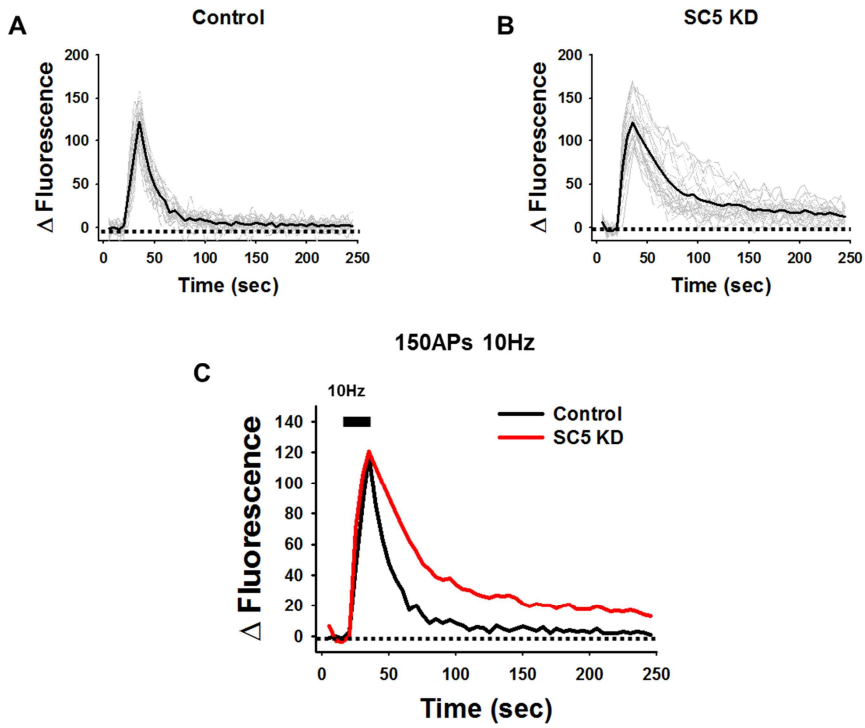

Figure 15. The pooled average fluorescence intensity showed the post-endocytic defects in SCAMP5 KD.

A and B, Average vGpH fluorescence intensity was measured from individual synapse on the control and SCAMP5 KD neurons. It was stimulated at 10 Hz for 15 s (150APs). Black line showed average response in neuron, a gray dashed line from a single synaptic bouton. (n=31 for control, n=33 for SC5 KD). **C**, Average fluorescence intensity got from the control and SCAMP5 KD neurons presented in A and B. Data are presented as means ± s.e. * $p < 0.01$ (Student's *t*-test).

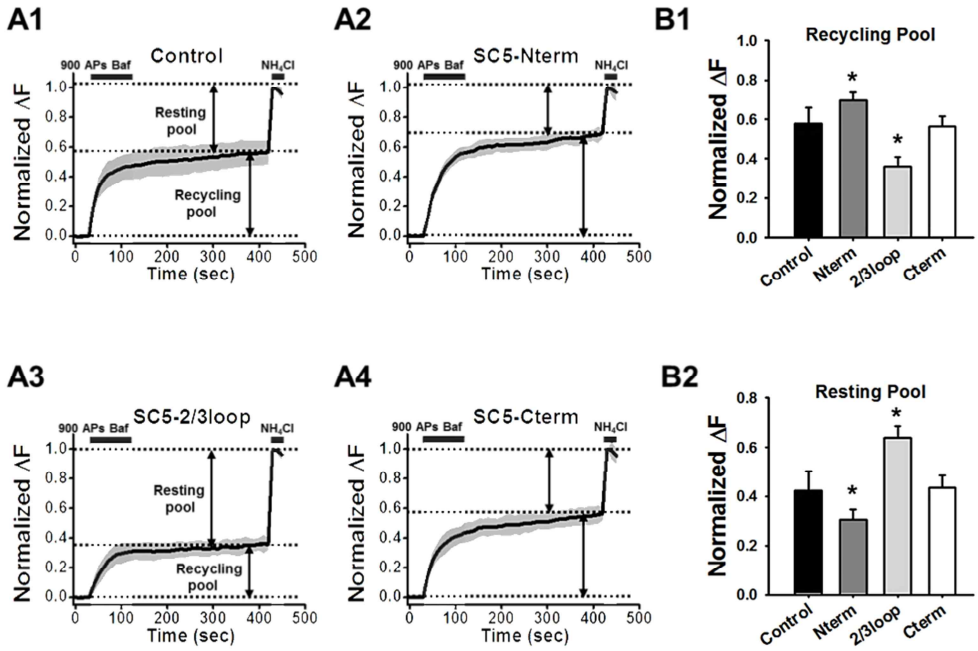

Figure 16. The ratio of recycling/resting pool size was significantly increased with SCAMP5-Nterm overexpression.

A1-A4, Average time course of vGpH fluorescence traces in control and SCAMP5 N-term, SCAMP5 2/3 loop, SCAMP5 C-term overexpressed neurons (n = 12 for control, n = 13 for SCAMP5 N-term, n = 15 SCAMP5 for 2/3 loop, n = 13 for SCAMP5 C-term) **B1-B2,** Average fraction values of recycling : resting pool for A1-A4 . 0.57 ± 0.08 : 0.42 ± 0.08 for control, 0.69 ± 0.04 : 0.31 ± 0.04 for SCAMP5 N-term, 0.36 ± 0.04 : 0.63 ± 0.04 for SCAMP5 2/3 loop, 0.56 ± 0.05 : 0.43 ± 0.05 for SCAMP5 C-term overexpressed neurons). Data are presented as means ± s.e. * $p < 0.01$ (Student's *t*-test).

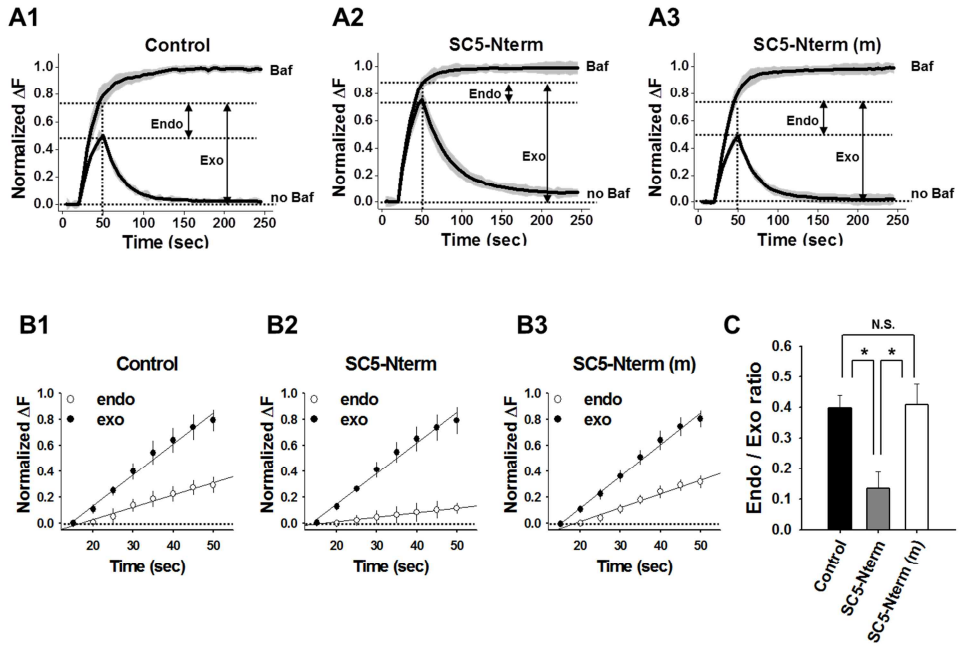

Figure 17. Overexpression of SCAMP5-Nterm severely impairs SV endocytosis during stimulation.

A1-A3, Average vGpH fluorescence intensity profiles from the control (A1), SCAMP5 N-term (A2), and SCAMP5 N-term mutant (A3) overexpressed neurons stimulated with or without *Baf*. Neurons were stimulated at 10 Hz for 30 s (300 APs) without *Baf*. After 10 min resting periods, the same neurons were stimulated again with 1,200 APs at 10 Hz in the presence of *Baf*. Fluorescence values were normalized to the maximal stable fluorescence signal in the *Baf* trace. (n = 12 for control, n = 13 for SCAMP5 N-term, n = 13 for SCAMP5 N-term mutant). **B1-3,** Graphs showing the time course of

endocytosis (Endo) and exocytosis (Exo) during stimulation with 300 APs at 10 Hz. The rate of exocytosis and endocytosis during stimulation were obtained from the linear fits to the initial 30 s of traces (exocytotic rate: 0.132 ± 0.04 for the control, 0.143 ± 0.05 for SCAMP5 N-term, 0.139 ± 0.06 for SCAMP55 N-term mutant; endocytic rate: 0.052 ± 0.04 for the control, 0.020 ± 0.04 for SCAMP5 N-term, 0.057 ± 0.05 for SCAMP5 N-term mutant). **C,** Ratios of endocytosis/exocytosis rate: 0.397 ± 0.04 for the control, 0.134 ± 0.05 for SCAMP5 N-term, 0.408 ± 0.04 for SCAMP5 N-term mutant. Data are presented as means ± s.e. * $p < 0.01$ (ANOVA and Tukey's HSD post hoc test).

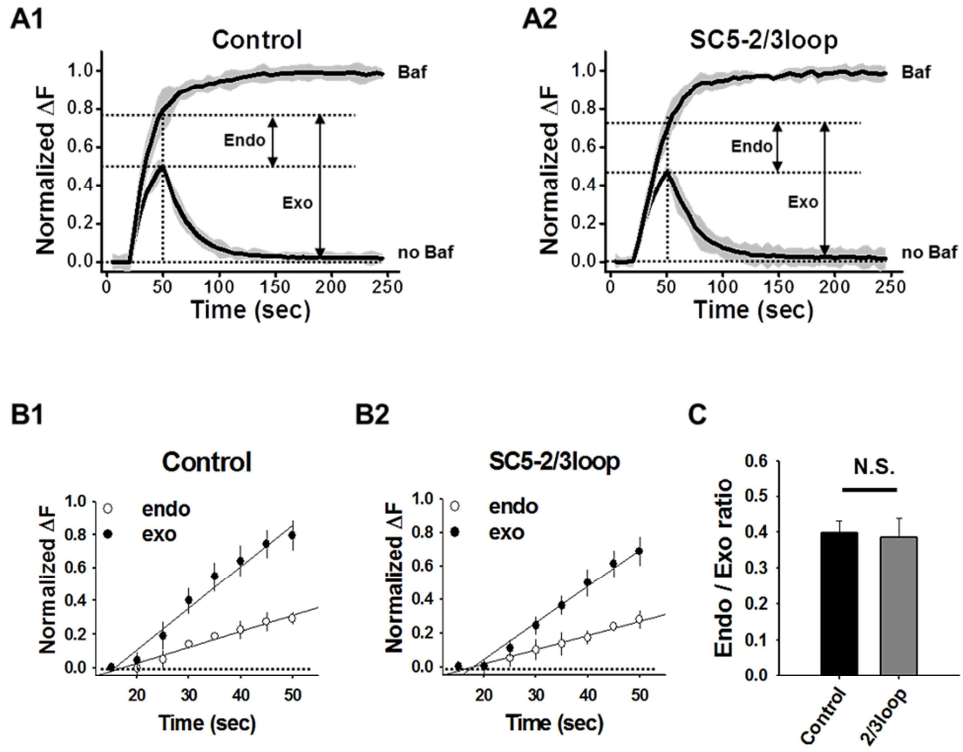

Figure 18. Overexpression of SCAMP5 2/3 loop does not affect the SV endocytosis during stimulation.

A1-A3, Average vGpH fluorescence intensity profiles from control (A1) and SCAMP5 2/3 loop (A2) overexpressed neurons stimulated with or without *Baf*. Fluorescence values were normalized to the maximal stable fluorescence signal in the *Baf* trace. (n = 15 for control, n = 14 for SCAMP5 2/3 loop). **B1-B2,** Graphs showing the time course of endocytosis (Endo) and exocytosis (Exo) during stimulation with 300 APs at 10 Hz. The rate of exocytosis and endocytosis during stimulation were obtained from the linear fits to the initial

30 s of traces (exocytotic rate: 0.133 ± 0.05 for the control, 0.118 ± 0.06 for SCAMP5 2/3 loop; endocytic rate: 0.052 ± 0.04 for the control, 0.045 ± 0.05 for SCAMP5 2/3 loop). **C,** Ratios of endocytosis/exocytosis rate: 0.397 ± 0.03 for the control, 0.386 ± 0.05 for SCAMP5 2/3 loop. Data are presented as means ± s.e. $p > 0.05$ (Student's *t*-test).

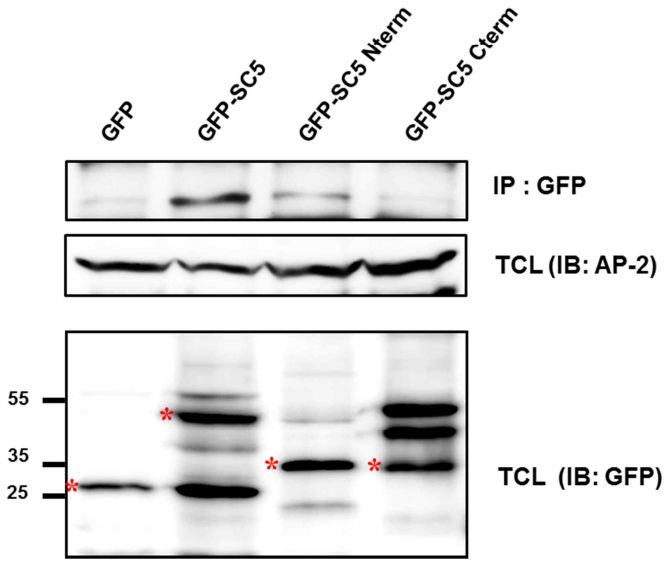

Figure 19. SCAMP5 binds to AP-2 through its N-terminal domain

In vitro binding assay of SCAMP5 and AP-2. HEK 293T cells transfected with GFP-SCAMP5, GFP-SCAMP5 N-term, GFP-SCAMP5 C-term constructs. After 72 h transfection, cells were lysed and immunoprecipitated with anti-GFP antibody to verified SCAMP5 and AP-2 interaction. Note that SCAMP5 binds to AP-2 via N-terminal domain.

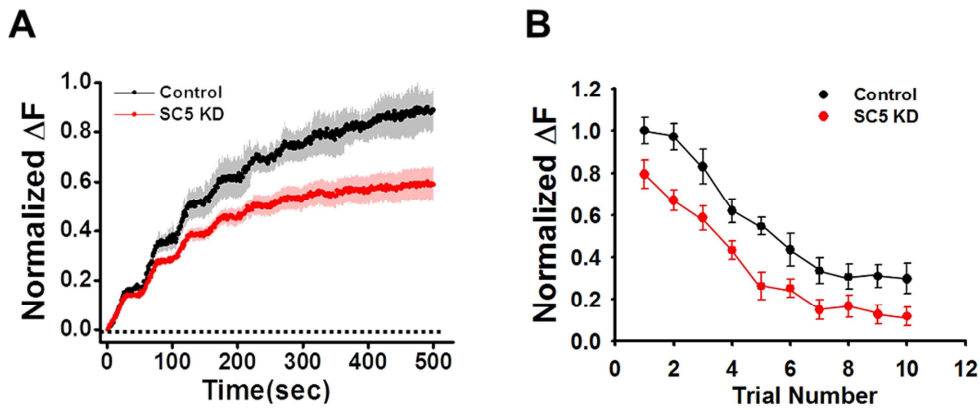

Figure 20. The depletion of fusion competent SVs during multiple stimuli was facilitated in SCAMP5 KD.

A, to reveal responses to consecutive stimuli, vGpH transfected neurons were incubated in *Baf* for 1min, after that the neurons were stimulated 40APs 20Hz, the same trial was repeated 10 times with 50sec interval in the presence of *Baf*. (Control : black line, SCAMP5 KD: red line). **B,** Plot shows the fluorescence change in each trial. In control almost maintain SV release at the last trial, whereas SCAMP5 KD the release of the SV was reduced compared with control. (29.79% ± 7.2% for control; 11.64% ± 4.3% for SC5 KD, n=5 for each). Data are presented as means ± s.e. * $p < 0.01$ (Student's *t*-test).

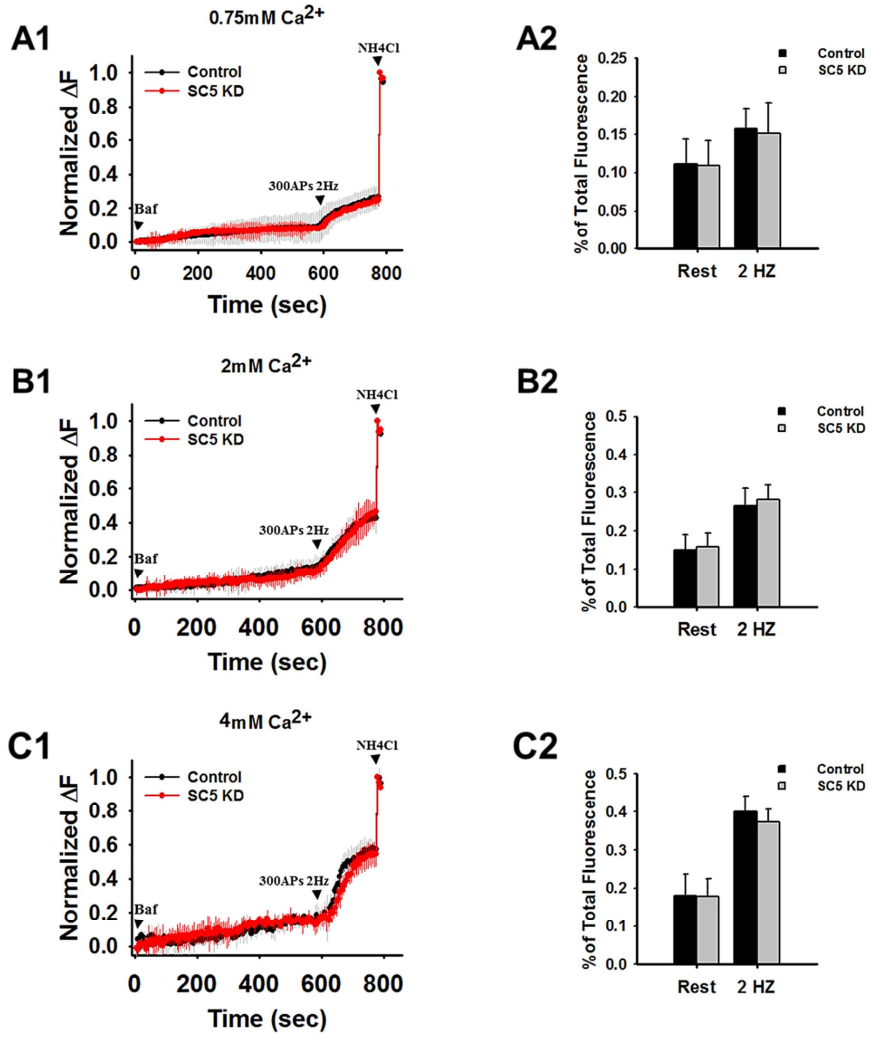

Figure 21. Spontaneous neurotransmission was not affected by the SCAMP5 KD.

A1, To monitor the spontaneous release, hippocampal neurons co-transfected with pU6mRFP-vector and vGpH (control); SCAMP5 shRNA and vGpH (SC5 KD). Neurons were imaged in the presence of 0.75mM $CaCl_2$ contained Tyrode and 0.5μm bafilomycin at unstimulated state (Rest) for 10min,

followed by stimulation with 2Hz for 150sec. Control and SC5 KD cells show, vGpH fluorescence similarly increased in Rest state. In 300APs 2Hz stimulated state, the vGpH fluorescence increase more than rest state. (n=8 for control, n=10 for SC5 KD). The total fluorescence can be observed after NH4Cl treatment. **A2,** Average data from the experiments showed in (A1). The increased fluorescence in unstimulated (Rest) and stimulated state has no statistical difference in SC5 KD. (Increased fluorescence and total fluorescence proportion. Rest: 0.11 ± 0.03 for control, 0.10 ± 0.03 for SC5 KD ; 2Hz stimulation 0.15 ± 0.03 for control, 0.15 ± 0.04 for SC5 KD). **B1 and B2,** The same experimental protocol used below and which in different $CaCl_2$ concentrations. Neurons incubated in 2mM $CaCl_2$ contained Tyrode. The fluorescence changed to show here (Increased fluorescence and total fluorescence proportion. Rest: 0.15 ± 0.03 for control, 0.15 ± 0.03 for SC5 KD ; 2Hz stimulation 0.26 ± 0.04 for control, 0.28 ± 0.03 for SC5 KD) have no significant difference. **C1 and C2,** Neurons incubated in 4mM $CaCl_2$ contained Tyrode. The fluorescence changed to show here (Increased fluorescence and total fluorescence proportion. Rest: 0.18 ± 0.05 for control, 0.17 ± 0.04 for SC5 KD ; 2Hz stimulation 0.39 ± 0.04 for control, 0.37 ± 0.03 for SC5 KD) also have no significant differences.

DISCUSSION

The key findings of the present study are that SCAMP5 is essential for maintaining the total SV pool size and SV endocytosis, which are important for compensating for ongoing exocytosis occurring during stimulation.

Most previous studies of the SCAMPs have focused on the regulation of exocytosis during dense-core vesicle (DCV) secretion or vesicle trafficking in the TGN. SCAMP1 plays a dual role in facilitating the dilation and closure of fusion pores and has been implicated in exo-endocytic coupling and in the regulation of DCV secretion in PC12 cells (20, 23, 63). SCAMP2 is known to interact with Arf6, phospholipase D1, and phosphatidylinositol 4,5-bisphosphate via its E-peptide 2/3 cytoplasmic loop domain (CWYRPIYKAFR) and to regulate fusion pore formation during DCV exocytosis (22, 24-26). It also interacts with the mammalian (Na^+, K^+)/H^+ exchanger, NHE7, in the TGN and participates in the shuttling of NHE7 between recycling vesicles and the TGN (27). The NPF repeats of SCAMP1 are also known to bind to two EH domain proteins: intersectin 1, which is involved in endocytic budding at the plasma membrane, and γ-synergin, which may mediate the budding of vesicles in the trans-Golgi complex (63). In addition, the expression of SCAMP1 without the N-terminal NPF repeats potently inhibits transferrin uptake by endocytosis (63).

Compared to other SCAMPs, however, less is known about the role of SCAMP5. One recent study showed that its expression is markedly increased in the striatum of HD disease patients and that its down-regulation alleviates

ER stress-induced protein aggregation in huntingtin mutants and the inhibition of endocytosis. Another study showed that human SCAMP5 directly interacts with synaptotagmins via its cytosolic C-terminal tail and is involved in the calcium-regulated exocytosis of signal peptide-containing cytokines (64). However, I found in this study that knock-down of SCAMP5 or overexpression of SCAMP5-Nterm caused endocytic defects during strong stimulation of cultured hippocampal neurons, whereas the exocytic kinetics were not affected. This difference in its effects on exocytosis could be due to mechanistic differences in exo-endocytosis between non-neuronal cells and neurons during intense stimulation. Unlike neurons, non-neuronal cells are never exposed to such strong activation *in vivo*. This explanation is consistent with the fact that KD synapses displayed little or no defects in endocytosis when stimulated at a low frequency (5 Hz). It seems that in SCAMP5 KD neurons, the endocytic capacity to cope with heavy exocytic loads is reduced, whereas the endocytosis activity of individual SVs during mild exocytic loads remains unaffected.

In addition, although I didn't find any defects in exocytosis in SCAMP5 KD synapses, I cannot completely rule out the possibility that SCAMP5 has an effect on exocytosis since the effect of SCAMP5 on single SV fusion kinetics was not tested. Instead, I tested the macroscopic kinetics of exocytosis upon sustained stimulation and this stimulation might mask subtle changes in unitary SV fusion kinetics.

Recent evidence suggests that endocytosis occurring during and after stimulation might have a distinct molecular mechanism (65). In this study, the

exo/endocytosis assay showed that endocytosis during stimulation (300 APs at 10 Hz) caused a severe defect in the SCAMP5 KD neurons, but that endocytosis after stimulation did not. From these results, I have therefore concluded that SCAMP5 may serve as a regulator of SV endocytosis during neuronal activity.

Although total SV pool size varies from bouton to bouton even in a single neuron, when compared to the control and SCAMP5 KD boutons of similar size, SCAMP5 KD resulted in a reduction of total SV pool size as well as of that of the recycling pool. The ratio of the recycling/resting pool size was, however, significantly increased. Moreover, the recruitment of reserve SVs during multiple stimuli (40 APs at 20 Hz, 10 times) was reduced in the SCAMP5 KD neurons, which indicates that SCAMP5 has a fast synaptic depression (Figure 20). This result is consisted with previous findings regarding the reduction of total SV pool size. The size of the recycled SV pools and the exo/endocytosis kinetics in the recycling pathways are known to play important roles in efficient synaptic function. In this study, since the endocytosis after stimulation was only moderately affected and the exocytosis kinetics were not affected by SCAMP5 KD, I speculate that the change in this ratio of the recycling/ resting pool size could be due to a compensatory mechanism that allows the neurons to maintain synaptic transmission during high levels of activity.

My results further suggest that SCAMP5 is essential when neuronal activity is high and a heavy endocytic load is imposed on the cell. This is reminiscent of a study on the selective requirement for dynamin-1 during high levels of

neuronal activity (65). Where the authors found that dynamin-1 was dispensable for the endocytic recycling of SVs but became essential when an intense stimulus imposed a heavy load on the endocytosis (65). In addition, a more recent study showed that synaptophysin knock-out (*syp-/-*) synapses exhibited defective SV endocytosis both during and after neuronal activity, while exocytosis and the size of the total recycling pool of SVs were unaffected (66). That study also found that *syp-/-* neurons displayed pronounced synaptic depression and slower recovery of the recycling SV pool after depletion. Interestingly, synaptophysin and SCAMP5, together with synaptogyrin, are tetraspan vesicle membrane proteins (TVPs) as they have four transmembrane regions and cytoplasmically-located termini and contribute to vesicle trafficking and membrane morphogenesis (67). Although previous studies have found little or no phenotypic defects in neurons of knockout mice lacking synaptophysin, synaptogyrin-1, or SCAMP1 (20, 68-70), my current data strongly suggest that the TVPs on SVs contribute to subtle neuronal functions such as the control of SV recycling during sustained neuronal activity.

More evidence suggests that synaptic dysfunction might be an initial stage in neurodegeneration, which is a progressive loss of neuronal structure or function (84, 85). Indeed, synaptic dysfunction is a common feature of neurodegenerative disease, including Parkinson's (PD), Alzheimer's disease (AD), and Huntington's disease (HD). For instance, mutation of the LRRK2 gene is linked to familial PD (73) and the overexpression of mutated LRRK2 is induced to decrease SV endocytosis and lower the rate of SV trafficking

(74). Synaptic dysfunctions are closely related to autism spectrum disorders (ASD) and other neuropsychiatric disorders, such as schizophrenia and intellectual disabilities (75). The synapsins have been found as the novel identified autism candidate gene. Synapsins are most abundant neuronal phosphoproteins that participate in synaptic transmission and plasticity (76). In addition, the deletion of synapsin isoforms (Syn1, Syn2*)* affects communication and social interactions and causes repetitive behaviors, resulting in autistic-like phenotypes (77).

Previous studies have reported that SCAMP5 shows high correlations with pathological conditions, notably neurological diseases, such as HD (29), ASD (37), ADHD (31-33), and some cancer-related conditions (34, 36). Such a high correlation between various neurological diseases and SCAMP5 expression imply its importance in nervous function but none has been reported so far.

Recent study discovered that SCAMP5 is another presynaptic candidate gene for autism (37). In addition, several autism candidate genes have recently been identified, including NLGN3, NLGN4, SHANK2/3, and IL1RAPL1 (which are coding for the postsynaptic protein) and CNTNAP2, RIMS3/NIM3, and SYN1/2 (which are cording for presynaptic proteins) (78, 79). Among these genes, Syn was found to play a role in the modulation of SV endocytosis; that is, it is recruited to the newly endocytosed SVs in the active zone (80). Another study showed that Syn interacts with intersectin to mediate SV recycling, which also contributes to during stimulation in the active zone (81). $Syn1^{-/-}$ mice have also showed a significant decrease in the

total number of SVs (83), and Syn1$^{-/-}$ cultured hippocampal neurons have a normal spontaneous neurotransmitter release (82). These studies have suggested that Syn1 is implicated in SV endocytosis and SV pool clustering, which play similar roles in synapse function. Based on these results, I hypothesize that SCAMP5 and Syn1 form a complex in the nerve terminal and that this interaction plays a critical role in presynaptic nerve terminals.

SCAMP5 does not contain an N-terminal NPF motif and is not known to directly interact with dynamin-1, but I have found that there are putative AP-2 binding sites (YXXϕ) in its N-terminus and 2/3 loop region. In additional, the IP assay showed that AP-2 binds to full-length SCAMP5 and the SCAMP5-Nterm domain but not to the SCAMP5-Cterm domain. Therefore, SCAMP5 may act as a molecular intermediate between Syn1 and AP-2 to allow for efficient retrieval of SVs endocytosis. In addition, SCAMP5 may directly or indirectly interact with dynamin-1 and other endocytic proteins to effectively accomplish endocytosis during intense stimulation. Further studies should focus on the molecular mechanisms through which SCAMP5 interacts with more other endocytic proteins to control SV recycling.

In conclusion, SCAMP5 functions to control the SV recycling machinery when neuronal activity is high enough to impose a heavy load on endocytosis. It may recruit or promote the assembly of endocytic components in order to neuronal activity. My data support recent suggestions that changes in the expression of SCAMP5 in Huntington's disease and autism may be related to the synaptic dysfunction observed in these patients.

REFERENCE

1. Takei K, Haucke V. Clathrin-mediated endocytosis: membrane factors pull the trigger. Trends Cell Biol 2001;11(9):385-391.

2. Schmid EM, McMahon HT. Integrating molecular and network biology to decode endocytosis. Nature 2007;448(7156):883-888.

3. Schmid EM, Ford MG, Burtey A, Praefcke GJ, Peak-Chew SY, Mills IG, Benmerah A, McMahon HT. Role of the AP2 beta-appendage hub in recruiting partners for clathrin-coated vesicle assembly. PLoS Biol 2006;4(9):e262.

4. Masuda M, Takeda S, Sone M, Ohki T, Mori H, Kamioka Y, Mochizuki N. Endophilin BAR domain drives membrane curvature by two newly identified structure-based mechanisms. EMBO J 2006;25(12):2889-2897.

5. Peter BJ, Kent HM, Mills IG, Vallis Y, Butler PJ, Evans PR, McMahon HT. BAR domains as sensors of membrane curvature: the amphiphysin BAR structure. Science 2004;303(5657):495-499.

6. Takei K, Slepnev VI, Haucke V, De Camilli P. Functional partnership between amphiphysin and dynamin in clathrin-mediated endocytosis. Nat Cell Biol 1999;1(1):33-39.

7. Itoh T, Erdmann KS, Roux A, Habermann B, Werner H, De Camilli P. Dynamin and the actin cytoskeleton cooperatively regulate plasma membrane invagination by BAR and F-BAR proteins. Dev Cell 2005;9(6):791-804.

8. Praefcke GJ, McMahon HT. The dynamin superfamily: universal membrane tubulation and fission molecules? Nat Rev Mol Cell Biol 2004;5(2):133-147.

9. Roux A, Uyhazi K, Frost A, De Camilli P. GTP-dependent twisting of dynamin implicates constriction and tension in membrane fission. Nature 2006;441(7092):528-531.

10. Farsad K, Ringstad N, Takei K, Floyd SR, Rose K, De Camilli P. Generation of high curvature membranes mediated by direct endophilin bilayer interactions. J Cell Biol 2001;155(2):193-200.

11. Cousin MA, Robinson PJ. The dephosphins: dephosphorylation by calcineurin triggers synaptic vesicle endocytosis. Trends Neurosci 2001;24(11):659-665.

12. Murthy VN, De Camilli P. Cell biology of the presynaptic terminal. Annu Rev Neurosci 2003;26:701-728.

13. Dittman J, Ryan TA. Molecular circuitry of endocytosis at nerve terminals. Annu Rev Cell Dev Biol 2009;25:133-160.

14. Granseth B, Odermatt B, Royle SJ, Lagnado L. Clathrin-mediated endocytosis: the physiological mechanism of vesicle retrieval at hippocampal synapses. J Physiol 2007;585(Pt 3):681-686.

15. Cingolani LA, Goda Y. Actin in action: the interplay between the actin cytoskeleton and synaptic efficacy. Nature Rev Neurosci 2008;9(5):344-356.

16. Fernandez-Chacon R, Sudhof TC. Novel SCAMPs lacking NPF repeats: Ubiquitous and synaptic vesicle-specific forms implicate SCAMPs in multiple membrane-trafficking functions. J Neurosci 2000;20(21):7941-7950.

17. Fernandez-Chacon R, Sudhof TC. Novel SCAMPs lacking NPF repeats: ubiquitous and synaptic vesicle-specific forms implicate SCAMPs in multiple membrane-trafficking functions. J Neurosci 2000;20(21):7941-7950.

18. Brand SH, Laurie SM, Mixon MB, Castle JD. Secretory carrier membrane proteins 31-35 define a common protein composition among secretory carrier membranes. J Biol chem 1991;266(28):18949-18957.

19. Brand SH, Castle JD. SCAMP 37, a new marker within the general cell surface recycling system. EMBO J 1993;12(10):3753-3761.

20. Fernandez-Chacon R, Alvarez de Toledo G, Hammer RE, Sudhof TC. Analysis of SCAMP1 function in secretory vesicle exocytosis by means of gene targeting in mice. J Biol Chem 1999;274(46):32551-32554.

21. Liao H, Zhang J, Shestopal S, Szabo G, Castle A, Castle D. Nonredundant function of secretory carrier membrane protein isoforms in dense core vesicle exocytosis. Am J Physiol Cell Physiol 2008;294(3):C797-809.

22. Guo ZH, Liu LX, Cafiso D, Castle D. Perturbation of a very late step of regulated exocytosis by a secretory carrier membrane protein (SCAMP2)-derived peptide. J Biol Chem 2002;277(38):35357-35363.

23. Zhang J, Castle D. Regulation of fusion pore closure and compound exocytosis in neuroendocrine PC12 cells by SCAMP1. Traffic 2011;12(5):600-614.

24. Liu LX, Guo ZH, Tieu QY, Castle A, Castle D. Role of secretory carrier membrane protein SCAMP2 in granule exocytosis. Mol Biol Cell 2002;13(12):4266-4278.

25. Liu LX, Liao HN, Castle A, Zhang J, Casanova J, Szabo G, Castle D. SCAMP2 interacts with Arf6 and phospholipase D1 and links their function to exocytotic fusion pore formation in PC12 cells. Mol Biol Cell 2005;16(10):4463-4472.

26. Liao H, Ellena J, Liu L, Szabo G, Cafiso D, Castle D. Secretory carrier membrane protein SCAMP2 and phosphatidylinositol 4,5-bisphosphate interactions in the regulation of dense core vesicle exocytosis. Biochemistry 2007;46(38):10909-10920.

27. Lin PJC, Williams WP, Luu Y, Molday RS, Orlowski J, Numata M. Secretory carrier membrane proteins interact and regulate trafficking of the organellar (Na+,K+)/H+ exchanger NHE7. J Cell Sci 2005;118(9):1885-1897.

28. Wu TT, Castle JD. Tyrosine phosphorylation of selected secretory carrier membrane proteins, SCAMP1 and SCAMP3, and association with the EGF receptor. Mol Biol Cell 1998;9(7):1661-1674.

29. Noh JY, Lee H, Song S, Kim NS, Im W, Kim M, Seo H, Chung CW, Chang JW, Ferrante RJ, Yoo YJ, Ryu H, Jung YK. SCAMP5 links endoplasmic reticulum stress to the accumulation of expanded polyglutamine protein aggregates via endocytosis inhibition. J Biol Chem 2009;284(17):11318-11325.

30. Heijtz RD, Alexeyenko A, Castellanos FX. Calcyon mRNA expression in the frontal-striatal circuitry and its relationship to vesicular processes and ADHD. Behav Brain Funct 2007;3:33.

31. Xiao J, Dai R, Negyessy L, Bergson C. Calcyon, a novel partner of clathrin light chain, stimulates clathrin-mediated endocytosis. J Biol Chem 2006;281(22):15182-15193.

32. Laurin N, Misener VL, Crosbie J, Ickowicz A, Pathare T, Roberts W, Malone M, Tannock R, Schachar R, Kennedy JL, Barr CL. Association of the calcyon gene (DRD1IP) with attention deficit/hyperactivity disorder. Molecular Psychiatry 2005;10(12):1117-1125.

33. Negyessy L, Bergson C, Garab S, Simon L, Goldman-Rakic PS. Ultrastructural localization of calcyon in the primate cortico-basal ganglia-thalamocortical loop. Neurosci Lett 2008;440(1):59-62.

34. Liu T, Papagiannakopoulos T, Puskar K, Qi S, Santiago F, Clay W, Lao K, Lee Y, Nelson SF, Kornblum HI, Doyle F, Petzold L, Shraiman B, Kosik KS. Detection of a microRNA signal in an in vivo expression set of mRNAs. PloS One 2007;2(8):e804.

35. Kisby GE, Standley M, Park T, Olivas A, Fei S, Jacob T, Reddy A, Lu X, Pattee P, Nagalla SR. Proteomic analysis of the genotoxicant methylazoxymethanol (MAM)-induced changes in the developing cerebellum. J Proteome Res 2006;5(10):2656-2665.

36. Taniwaki M, Daigo Y, Ishikawa N, Takano A, Tsunoda T, Yasui W, Inai K, Kohno N, Nakamura Y. Gene expression profiles of small-cell lung cancers: molecular signatures of lung cancer. Int J Oncol 2006;29(3):567-575.

37. Castermans D, Volders K, Crepel A, Backx L, De Vos R, Freson K, Meulemans S, Vermeesch JR, Schrander-Stumpel CTRM, De Rijk P, Del-Favero J, Van Geet C, Van De Ven WJM, Steyaert JG, Devriendt K*, et al.* SCAMP5, NBEA and AMISYN: three candidate genes for autism involved in secretion of large dense-core vesicles. Hum Mol Genet 2010;19(7):1368-1378.

38. Motley A, Bright NA, Seaman MN, Robinson MS. Clathrin-mediated endocytosis in AP-2-depleted cells. J Cell Biol 2003;162(5):909-918.

39. Boucrot E, Saffarian S, Zhang R, Kirchhausen T. Roles of AP-2 in clathrin-mediated endocytosis. PloS One 2010;5(5):e10597.

40. Chang S, De Camilli P. Glutamate regulates actin-based motility in axonal filopodia. Nat Neurosci 2001;4(8):787-793.

41. Lee S, Lee K, Hwang S, Kim SH, Song WK, Park ZY, Chang S. SPIN90/WISH interacts with PSD-95 and regulates dendritic spinogenesis via an N-WASP-independent mechanism. EMBO J 2006;25(20):4983-4995.

42. Burrone J, Li ZY, Murthy VN. Studying vesicle cycling in presynaptic terminals using the genetically encoded probe synaptopHluorin. Nat Protoc 2006;1(6):2970-2978.

43. Sankaranarayanan S, De Angelis D, Rothman JE, Ryan TA. The use of pHluorins for optical measurements of presynaptic activity. Biophys J 2000;79(4):2199-2208.

44. Voglmaier SM, Kam K, Yang H, Fortin DL, Hua Z, Nicoll RA, Edwards RH. Distinct endocytic pathways control the rate and extent of synaptic vesicle protein recycling. Neuron 2006;51(1):71-84.

45. Murthy VN, Sejnowski TJ, Stevens CF. Heterogeneous release properties of visualized individual hippocampal synapses. Neuron 1997;18(4):599-612.

46. Trommershauser J, Schneggenburger R, Zippelius A, Neher E. Heterogeneous presynaptic release probabilities: functional relevance for short-term plasticity. Biophys J 2003;84(3):1563-1579.

47. Balaji J, Armbruster M, Ryan TA. Calcium control of endocytic capacity at a CNS synapse. J Neurosci 2008;28(26):6742-6749.

48. Fernandez-Alfonso T, Ryan TA. The kinetics of synaptic vesicle pool depletion at CNS synaptic terminals. Neuron 2004;41(6):943-953.

49. Hua Z, Leal-Ortiz S, Foss SM, Waites CL, Garner CC, Voglmaier SM, Edwards RH. v-SNARE composition distinguishes synaptic vesicle pools. Neuron 2011;71(3):474-487.

50. Ramirez DM, Khvotchev M, Trauterman B, Kavalali ET. Vti1a identifies a vesicle pool that preferentially recycles at rest and maintains spontaneous neurotransmission. Neuron 2012;73(1):121-134.

51. Granseth B, Lagnado L. The role of endocytosis in regulating the strength of hippocampal synapses. J Physiol 2008;586(Pt 24):5969-5982.

52. Sankaranarayanan S, Ryan TA. Real-time measurements of vesicle-SNARE recycling in synapses of the central nervous system. Nat Cell Biol 2000;2(4):197-204.

53. Ryan TA, Reuter H, Wendland B, Schweizer FE, Tsien RW, Smith SJ. The kinetics of synaptic vesicle recycling measured at single presynaptic boutons. Neuron 1993;11(4):713-724.

54. Ohno H, Aguilar RC, Yeh D, Taura D, Saito T, Bonifacino JS. The medium subunits of adaptor complexes recognize distinct but overlapping sets of tyrosine-based sorting signals. J Biol Chem 1998;273(40):25915-25921.

55. Ohno H, Stewart J, Fournier MC, Bosshart H, Rhee I, Miyatake S, Saito T, Gallusser A, Kirchhausen T, Bonifacino JS. Interaction of tyrosine-based sorting signals with clathrin-associated proteins. Science 1995;269(5232):1872-1875.

56. Owen DJ, Evans PR. A structural explanation for the recognition of tyrosine-based endocytotic signals. Science 1998;282(5392):1327-1332.

57. Sabatini BL, Regehr WG. Timing of synaptic transmission. Annu Rev Physiol 1999;61:521-542.

58. Arellano JI, Espinosa A, Fairen A, Yuste R, DeFelipe J. Non-synaptic dendritic spines in neocortex. Neuroscience 2007;145(2):464-469.

59. Engert F, Bonhoeffer T. Dendritic spine changes associated with hippocampal long-term synaptic plasticity. Nature 1999;399(6731):66-70.

60. Maletic-Savatic M, Malinow R, Svoboda K. Rapid dendritic morphogenesis in CA1 hippocampal dendrites induced by synaptic activity. Science 1999;283(5409):1923-1927.61.

61. Yuste R, Majewska A. On the function of dendritic spines. The Neuroscientist 2001;7(5):387-395.

62. Kaufmann WE, Moser HW. Dendritic anomalies in disorders associated with mental retardation. Cerebral Cortex 2000;10(10):981-991.

63. Fernandez-Chacon R, Achiriloaie M, Janz R, Albanesi JP, Sudhof TC. SCAMP1 function in endocytosis. J Biol Chem 2000;275(17):12752-12756.

64. Han CF, Chen TY, Yang MJ, Li N, Liu HB, Cao XT. Human SCAMP5, a Novel Secretory Carrier Membrane Protein, Facilitates Calcium-Triggered Cytokine Secretion by Interaction with SNARE Machinery. J Immunol 2009;182(5):2986-2996.

65. Ferguson SM, Brasnjo G, Hayashi M, Wolfel M, Collesi C, Giovedi S, Raimondi A, Gong LW, Ariel P, Paradise S, O'Toole E, Flavell R, Cremona O, Miesenbock G, Ryan TA*, et al.* A selective activity-dependent requirement for dynamin 1 in synaptic vesicle endocytosis. Science 2007;316(5824):570-574.

66. Kwon SE, Chapman ER. Synaptophysin regulates the kinetics of synaptic vesicle endocytosis in central neurons. Neuron 2011;70(5):847-854.

67. Hubner K, Windoffer R, Hutter H, Leube RE. Tetraspan vesicle membrane proteins: synthesis, subcellular localization, and functional properties. Int Rev Cytol 2002;214:103-159.

68. Eshkind LG, Leube RE. Mice lacking synaptophysin reproduce and form typical synaptic vesicles. Cell Tissue Res 1995;282(3):423-433.

69. McMahon HT, Bolshakov VY, Janz R, Hammer RE, Siegelbaum SA, Sudhof TC. Synaptophysin, a major synaptic vesicle protein, is not essential for neurotransmitter release. Proc Natl Acad Sci USA 1996;93(10):4760-4764.

70. Janz R, Sudhof TC, Hammer RE, Unni V, Siegelbaum SA, Bolshakov VY. Essential roles in synaptic plasticity for synaptogyrin I and synaptophysin I. Neuron 1999;24(3):687-700.

71. Pang ZP, Sudhof TC. Cell biology of Ca^{2+}-triggered exocytosis. Curr Opin Cell Biol 2010;22(4):496-505.

72. Xu J, Pang ZP, Shin OH, Sudhof TC. Synaptotagmin-1 functions as a $Ca2^{+}$ sensor for spontaneous release. Nat Neurosci 2009;12(6):759-766.

73. Paisan-Ruiz C, Jain S, Evans EW, Gilks WP, Simon J, van der Brug M, Lopez de Munain A, Aparicio S, Gil AM, Khan N, Johnson J, Martinez JR, Nicholl D, Carrera IM, Pena AS, et al. Cloning of the gene containing mutations that cause PARK8-linked Parkinson's disease. Neuron 2004;44(5):595-600.

74. Xiong Y, Coombes CE, Kilaru A, Li X, Gitler AD, Bowers WJ, Dawson VL, Dawson TM, Moore DJ. GTPase activity plays a key role in the pathobiology of LRRK2. PLoS Genet 2010;6(5):e1000902.

75. Pinto D, Delaby E, Merico D, Barbosa M, Merikangas A, Klei L, Thiruvahindrapuram B, Xu X, Ziman R, Wang Z, Vorstman JA, Thompson A, Regan R, Pilorge M, Pellecchia G, et al. Convergence of genes and cellular pathways dysregulated in autism spectrum disorders. Am J Hum Genet 2014;94(5):677-694.

76 Fornasiero EF, Bonanomi D, Benfenati F, Valtorta F. The role of synapsins in neuronal development. Cell Mol Life Sci 2010;67(5):1383-1396.

77. Greco B, Manago F, Tucci V, Kao HT, Valtorta F, Benfenati F. Autism-related behavioral abnormalities in synapsin knockout mice. Behav Brain Res 2013;251:65-74.

78. Lignani G, Raimondi A, Ferrea E, Rocchi A, Paonessa F, Cesca F, Orlando M, Tkatch T, Valtorta F, Cossette P, Baldelli P, Benfenati F. Epileptogenic Q555X SYN1 mutant triggers imbalances in release dynamics and short-term plasticity. Hum Mol Genet 2013;22(8):2186-2199.

79. Fassio A, Patry L, Congia S, Onofri F, Piton A, Gauthier J, Pozzi D, Messa M, Defranchi E, Fadda M, Corradi A, Baldelli P, Lapointe L, St-Onge J, Meloche C, et al. SYN1 loss-of-function mutations in autism and partial epilepsy cause impaired synaptic function. Hum Mol Genet 2011;20(6):2297-2307.

80. Chi P, Greengard P, Ryan TA. Synapsin dispersion and reclustering during synaptic activity. Nat Neurosci 2001;4(9):1187-1193.

81. Evergren E, Gad H, Walther K, Sundborger A, Tomilin N, Shupliakov O. Intersectin is a negative regulator of dynamin recruitment to the synaptic endocytic zone in the central synapse. J Neurosci 2007;27(10):379-390.

82. Baldelli P, Fassio A, Valtorta F, Benfenati F. Lack of synapsin I reduces the readily releasable pool of synaptic vesicles at central inhibitory synapses. J Neurosci 2007;27(11):13520-13531.

83. Rosahl TW, Spillane D, Missler M, Herz J, Selig DK, Wolff JR, Hammer RE, Malenka RC, Sudhof TC. Essential functions of synapsins I and II in synaptic vesicle regulation. Nature 1995;375(12):488-493.

84. Waites CL, Garner CC. Presynaptic function in health and disease. Trends Neurosci 2011;34(13):326-337.

85. Spooren W, Lindemann L, Ghosh A, Santarelli L. Synapse dysfunction in autism: a molecular medicine approach to drug discovery in neurodevelopmental disorders. Trends Pharmacol Sci 2012;33(12):669-684.

Abstract in Korean(국문 초록)

신경전달물질은 신경세포에서 분비되는 신호물질로서, 신경세포에 자극이 전달되면 시냅스낭은 신경세포의 세포막으로 이동한다. 세포막으로 이동한 시냅스낭은 세포외 유출에 의해 신경전달물질을 시냅스로 방출시키고, 시냅스낭의 재생성 및 세포내 유입을 통해 지속적인 신경전달을 유지하게 된다. 시냅스에서는 시냅스 신호전달 관련 시냅스낭 단백질들이 신경계 신호전달, 시냅스 가소성, 항상성 조절에 관여하지만 그 단백질들의 정확한 기능에 관한 연구가 부족하다.

시냅스낭에 존재하는 단백질인 SCAMP5 는 시냅스낭 막을 네번 관통한 구조를 가지고 있으며, N-term, TM (1-4), C-term 도메인 구조를 가지고 있다. 지금까지 알려진 SCAMPs 는 모두 5 가지 아형으로서 SCAMP1-4는 여러 조직에 광범위하게 존재하는 반면 SCAMP5 는 뇌조직에 많이 존재하며 시냅스낭에 많이 존재하는 단백질이다. SCAMP1-3은 PC12세포에서 dense-core vesicle (DCV), 후기골지망(TGN), 엔도솜, 소포체의 이동 과정에 중요하게 관여한다.

최근 보고에 의하면 자폐증환자에서 SCAMP5의 발현양이 40%이하로 감소하였으며, 헌팅턴병 환자에서는 그 발현양이

증가하였다. 신경계 질병에서 SCAMP5의 발현양의 변화는 시냅스 기능의 이상을 유발하지만, 지금까지의 연구에서 그 정확한 기능에 대한 증거는 부족했다.

본 연구에서는 시냅스 전세포 말단에서의 SCAMP5의 정확한 기능을 밝히고자 연구를 진행하였다. SCAMP5-shRNA을 체외 배양된 쥐 해마신경세포에 처리하여 SCAMP5의 발현이 저하되면, total vesicle pool size 및 recycling pool size가 감소하고, recycling/resting pool 구성비율이 유의하게 증가하였다. 강한 전기자극이 주어지면 시냅스낭 세포내유입 과정이 현저히 느려지는 것을 관찰할 수 있었으며, FM1-43을 이용한 세포내 유입 실험에서도 동일한 결과를 관찰하였다. 강한 전기적 자극에 의해 세포외 유출이 증가하면, SCAMP5 발현이 저하된 신경세포에서는 자극동안에 세포내 유입이 느려짐으로, 자극에 의한 지속적인 시냅스낭의 세포외유출은 시냅스낭 세포내유입을 통한 시냅스낭의 재유입 및 순환을 유지하지 못하였다.

SCAMP5의 정확한 기능을 밝히기 위해, SCAMP5 단백질의 N-term, 2/3loop, C-term 도메인을 과발현한 결과, N-term 도메인을 과발현 하면 자극동안과 자극후의 세포내유입이 현저히 느려졌다. 이 결과는 SCAMP5 발현을 억제하였을 때의 결과와 유사하게 작용하였다. 실험결과 SCAMP5는 N-term 도메인의

YXXΦ 도메인을 통해 AP-2 단백질과 결합하여 시냅스낭의 순환과정에 관여함을 증명하였다.

본 연구를 통해 SCAMP5가 강한 신경자극이 전달될 때 시냅스낭 재순환 과정을 조절하는 기능을 가지며, 시냅스 활동도 즉 시냅스의 주요 기능인 신경전달 과정에 문제가 발생하는 것과 발달성 뇌장애인 자폐증 및 신경계 질병 헌팅턴병과 밀접한 연관성이 있음을 제시하였다.

주요어 : 신경활성상태, recycling pool, resting pool, SCAMP5, 시냅스낭 세포내유입.

학번 : 2010-24179